An Extended Compartmental Model for Divorce Dynamics with Reconciliation, Counseling, and Socioeconomic Factors

Abstract

This paper develops an extended mathematical framework for the analysis of divorce dynamics within a structured population. The proposed model is formulated as a linear inhomogeneous deterministic seven-compartment system that characterizes transitions among single, married, estranged, divorced, reconciled, counseling, and other related social states. Unlike many existing nonlinear social models, the present formulation admits explicit analytical tractability while incorporating behavioral control parameters that capture the effects of financial stress, social support, and digital media influence. The total population is rigorously shown to remain bounded, thereby ensuring positivity and invariance of the feasible region. Explicit closed-form expressions for the equilibrium states are derived, together with a divorce reproduction threshold parameter, $\mathcal{R}_d$, which governs the persistence or eradication of divorce dynamics. In particular, the divorce-free equilibrium is proven to be locally asymptotically stable when $\mathcal{R}_d < 1$ and unstable when $\mathcal{R}_d > 1$, thereby establishing a clear threshold condition for long-term marital stability. Stability properties are established through eigenvalue analysis of the associated system matrix and are further substantiated via Lyapunov-based arguments and parametric sensitivity analysis. Numerical simulations implemented using a fourth-order Runge–Kutta scheme validate the theoretical findings and demonstrate the stabilizing influence of reconciliation mechanisms and enhanced social support interventions. Overall, the study provides a mathematically rigorous and analytically tractable framework for understanding divorce persistence and offers quantitative insights that may inform evidence-based social and policy interventions.

Keywords: Divorce dynamics; Compartmental modeling; Nonlinear dynamical systems; Reproduction number $\mathcal{R}_d$; Stability analysis; Lyapunov methods; Sensitivity analysis.

1 Introduction

Human beings are inherently social by nature and, owing to intrinsic social tendencies and contextual circumstances, exist within structured communities. Among the most fundamental social institutions is marriage, which formalizes the interpersonal union between a man and a woman within biological, social, cultural, and legal frameworks. The legal characterization of marriage varies across juridical systems, being regarded as a sacrament under Hindu law and as a contractual arrangement under Muslim law. As the institution of marriage evolved over time, the concept of divorce emerged correspondingly. In contemporary legal terminology, divorce is defined as the formal dissolution of marriage, terminating the mutual rights and obligations of spouses. Although marriage has existed across civilizations, the recognition and regulation of divorce have historically been shaped by prevailing religious doctrines, cultural traditions, and legal principles. Early notions of separation appear in Indian mythology, notably in the *Ramayana*, where King Rama abandons Sita. Ancient legal systems also addressed marital dissolution; for instance, the Code of Hammurabi (c. 1754 BCE) permitted divorce under specified conditions, often favoring male authority, while Roman law allowed comparatively liberal provisions, including divorce by mutual consent. During the medieval era, under the profound influence of Christianity, marriage was widely regarded as indissoluble, and divorce was largely proscribed. The modern legal framework governing divorce gradually developed during the eighteenth and nineteenth centuries, paralleling the rise of secular legal systems that emphasized individual autonomy, civil rights, and legal equality.

In contemporary society, divorce is widely acknowledged as a legal remedy for irretrievably broken marriages and is shaped by a complex interplay of socioeconomic, psychological, cultural, and institutional determinants. Mathematical modeling offers a systematic and quantitative framework for examining these multifaceted interactions, thereby generating evidence-based insights to inform social planning and policy formulation. Empirical studies report increasing divorce rates in regions such as the United States, England and Wales, Spain, and several African countries [1, 2, 3, 4], with particularly pronounced growth observed in sub-Saharan Africa, especially among younger couples [5]. Recent theoretical investigations have further deepened the mathematical understanding of marital instability. For example, [6] proposed a nonlinear divorce model incorporating a fear-effect mechanism and performed bifurcation and stability analyses to identify critical threshold dynamics. Likewise, [7] formulated an age-structured nonlinear framework that integrates extra-marital influences and long-distance relational effects, illustrating how nonlinear interactions reshape equilibrium configurations and stability properties.

The social and developmental consequences of divorce have been extensively documented in the literature, particularly regarding its psychological and behavioral impacts on children [8, 9]. From a mathematical standpoint, divorce dynamics have also been examined through compartmental and epidemic-type modeling frameworks, highlighting structural analogies between social transition processes and disease transmission mechanisms [11]. Foundational theoretical developments in threshold analysis and reproduction number theory, originally formulated within epidemiological modeling [12, 13, 14], furnish rigorous analytical tools for investigating stability, persistence, and bifurcation phenomena in structured divorce systems. In addition, recent fuzzy and hybrid modeling paradigms have expanded the analytical landscape of marriage–divorce dynamics [10], providing flexible methodologies for incorporating uncertainty, imprecision, and social heterogeneity into deterministic population-based models.

Divorce dynamics are governed by the interaction of stabilizing and destabilizing forces within the marital system. Among the principal stabilizing mechanisms are reconciliation and counselling. Reconciliation operates as a multifactorial stabilizing process that restores marital equilibrium through emotional repair, social support, legal mediation, and behavioral adjustment. From a dynamical systems perspective, reconciliation increases the reconciliation rate γ, decreases the effective divorce rate δ, reduces the relapse probability ρ, and may lower the divorce reproduction threshold $\mathcal{R}_d$. As a consequence, it can introduce nonlinear resistance effects and, under specific parameter regimes, give rise to bistability phenomena. Counselling functions as an adaptive intervention mechanism that disrupts the progression from marital distress to dissolution by providing psychological, legal, and social guidance. It attenuates distress transition rates, strengthens reconciliation flows, and may shift the system below the critical threshold condition $\mathcal{R}_d < 1$. Such transitions can modify the long-term qualitative dynamics of the model, potentially inducing stability switching or bifurcation behavior. In contrast, socioeconomic conditions act as exogenous stress drivers that destabilize marital stability. Financial instability, unemployment, debt burden, income inequality, housing insecurity, migration pressures, and work–life imbalance intensify relational conflict and erode resilience. Mathematically, these stressors increase the conflict amplification parameter α, elevate the relapse probability ρ, and raise effective divorce transition rates, thereby promoting systemic instability. Hence, the long-term structural behavior of the marital system is determined by the dynamic interplay between stabilizing controls, such as reconciliation and counselling, and destabilizing socioeconomic pressures.

Recent studies continue to enrich the mathematical understanding of divorce dynamics by integrating behavioral, demographic, and structural complexities. For example, Pippal and Ranga (2025) developed an age-structured nonlinear compartmental model that captures transitions among stable marriage, long-distance relationships, extra-marital affairs, and divorce, revealing how behavioral parameters and age-dependent engagement influence equilibrium stability and bifurcation behavior [23]. Chang *et al.* (2024) introduced a nonlinear differential equation model based on real-world data to investigate divorce dynamics and elimination strategies, providing rigorous stability and sensitivity analyses [24]. Buxay *et al.* (2026) examined the role of tolerance in marital stability, demonstrating that increased tolerance is associated with lower divorce reproduction numbers and enhanced stability of the divorce-free equilibrium [25]. Additionally, Padder *et al.* (2025) combined ordinary differential equation modeling with statistical hypothesis testing to achieve highly accurate empirical fits to longitudinal divorce data, underscoring the value of integrating quantitative models with statistical validation [26]. These contemporary contributions highlight the ongoing evolution of mathematical frameworks that bridge theoretical analysis and empirical insights into divorce phenomena.

1.1 Reconciliation, Counselling, and Socio-Economic Determinants in Divorce Dynamics

Reconciliation, counselling, and socio-economic conditions constitute fundamental determinants of divorce dynamics within structured populations. Reconciliation refers to the restoration of marital relationships following conflict or separation and is frequently encouraged prior to formal legal dissolution. It preserves family cohesion, promotes emotional stability, safeguards children's psychological well-being, reduces legal and financial costs, and enhances long-term relational resilience. When conflicts are situational rather

than structural, reconciliation can substantially mitigate divorce incidence by improving communication and conflict-resolution capacity. From a mathematical perspective, reconciliation functions as a stabilizing mechanism represented by a reconciliation rate parameter that transfers individuals from estranged or conflict states back to a stable marital compartment, thereby reducing systemic instability. Similarly, counselling operates as a structured intervention strategy aimed at resolving interpersonal discord through pre-marital guidance, marital therapy, family mediation, or court-mandated processes. Counselling enhances emotional regulation, strengthens communication patterns, identifies underlying stressors such as financial strain or incompatibility, and discourages impulsive dissolution decisions. Within a dynamical systems framework, it may be modeled as a control parameter that decreases transition rates from married to divorced compartments while simultaneously increasing reconciliation probabilities. In contrast, socio-economic factors frequently act as exogenous destabilizing forces. Financial instability, unemployment, income disparities, urbanization, modernization, women's economic independence, educational attainment, and prevailing cultural and legal norms significantly influence marital stability. Economic hardship often amplifies marital conflict, whereas financial autonomy may increase the practical feasibility of divorce. Higher educational attainment may delay early dissolution through informed decision-making, yet it may also reinforce personal autonomy. Urban environments, characterized by mobility and modernization, typically exhibit higher divorce prevalence than rural settings. Consequently, the long-term qualitative behavior of divorce systems emerges from the dynamic interplay between stabilizing interventions and socio-economic stress drivers.

1.2 Motivation and Novelty of the Study

The increasing complexity of marital instability in contemporary societies necessitates a rigorous quantitative framework capable of integrating demographic, behavioral, and socioeconomic dimensions within a unified analytical structure. Although previous investigations have explored divorce dynamics using compartmental or nonlinear formulations, many existing models either concentrate on isolated behavioral factors or neglect explicit stabilizing control mechanisms such as reconciliation and counselling. Moreover, several demographic analyses remain largely descriptive and do not provide threshold-based criteria for assessing long-term structural stability. The present study is therefore motivated by the need to address these limitations through the development of an extended multi-compartment dynamical system that systematically incorporates reconciliation dynamics, counselling interventions, and socioeconomic stress parameters within a coherent mathematical framework. By embedding these mechanisms into a system of differential equations, the model permits rigorous examination of existence, boundedness, equilibrium structure, and stability transitions. The novelty of this work resides in three principal contributions: first, it explicitly integrates both stabilizing (reconciliation and counselling) and destabilizing (socioeconomic stress) mechanisms within a structured compartmental model, enabling direct analytical comparison of their competing effects; second, it derives a divorce reproduction threshold $\mathcal{R}_d$ via the next-generation matrix approach, thereby establishing a precise parameter-dependent criterion for marital persistence or dissolution; and third, it conducts a comprehensive stability and sensitivity analysis to quantify how intervention efficacy and socioeconomic stressors reshape the qualitative dynamics of the system. Unlike purely descriptive or empirically confined studies, the proposed framework offers a mathematically rigorous and policy-relevant formulation that bridges

social interpretation with dynamical systems theory, thereby strengthening both theoretical insight and practical applicability within the mathematical social sciences.

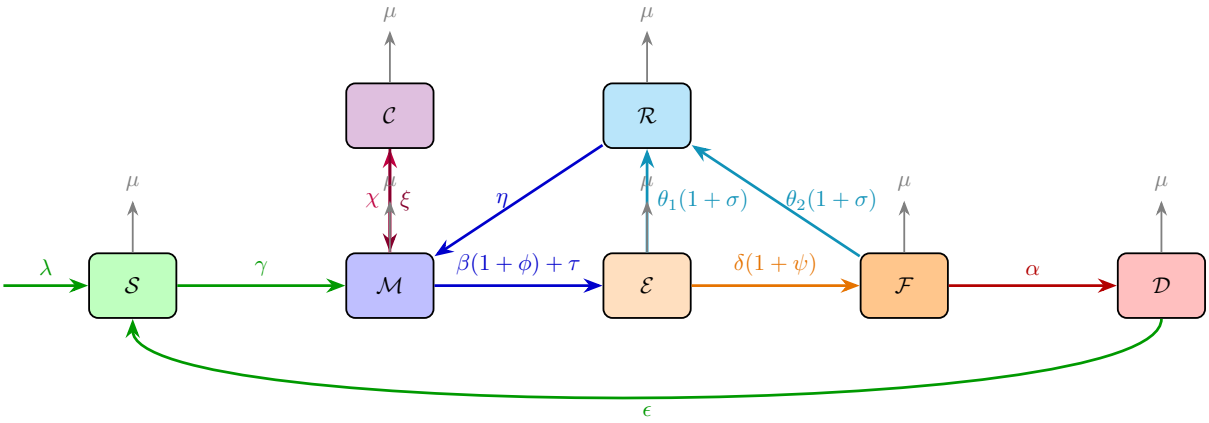

Figure 1: State transition diagram for the divorce–relationship dynamics model. Behavioral parameters ϕ (financial stress), σ (social support), and ψ (social media influence) act as external modifiers of selected transition rates rather than independent state variables.

2 Mathematical Model and Preliminaries

We formulate an extended compartmental model describing divorce dynamics under demographic, social, and behavioral influences. The population is partitioned into seven interacting compartments $\mathcal{S}, \mathcal{M}, \mathcal{E}, \mathcal{F}, \mathcal{D}, \mathcal{R}, \mathcal{C}$, with transitions governed by parameters $(\lambda, \mu, \gamma, \beta, \tau, \delta, \alpha, \epsilon, \theta_1, \theta_2, \eta, \chi, \xi)$ representing recruitment, natural removal, marriage, separation, conflict escalation, divorce, reconciliation, and counselling effects. A detailed parameter description is given in Table 1.
Behavioral influence indices (ϕ, σ, ψ) represent financial stress, social support, and social media effects, respectively. Since direct empirical estimates are unavailable, they are modeled as dimensionless control parameters satisfying

$$0 \leq \phi, \sigma, \psi \leq 1,$$

facilitating sensitivity and bifurcation analysis across diverse social environments.

2.1 Preliminaries

Consider the linear system

$$\dot{\mathbf{X}} = \mathbf{b} + \mathbf{A}\mathbf{X}, \qquad \mathbf{X} \in \mathbb{R}^7.$$

Lemma 2.1. *Let $\mathbf{X}^*$ be an equilibrium. The Lyapunov exponents are*

$$\Lambda_i = \Re(\lambda_i), \quad i = 1, \ldots, 7,$$

where λ_i are the eigenvalues of $\mathbf{A}$. The largest exponent is $\Lambda_{\max} = \max_i \Re(\lambda_i)$.

Theorem 2.2. *The equilibrium $\mathbf{X}^*$ is exponentially stable if $\Lambda_{\max} < 0$ and unstable if $\Lambda_{\max} > 0$.*

Theorem 2.3 (Global Exponential Stability)**.** *If all eigenvalues of* $\mathbf{A}$ *satisfy* $\Re(\lambda_i) < 0$*, then* $\mathbf{X}^*$ *is globally exponentially stable in* $\mathbb{R}^7$*, i.e.,*

$$\|\mathbf{X}(t) - \mathbf{X}^*\| \leq Me^{-\omega t}\|\mathbf{X}(0) - \mathbf{X}^*\|, \quad t \geq 0,$$

for some $M, \omega > 0$*.*

Proof. Let $\mathbf{Y} = \mathbf{X} - \mathbf{X}^*$, so that $\dot{\mathbf{Y}} = \mathbf{A}\mathbf{Y}$. If $\Re(\lambda_i) < 0$, then $\mathbf{A}$ is Hurwitz. Hence, for $\mathbf{Q} = \mathbf{I}$, there exists $\mathbf{P} > 0$ satisfying

$$\mathbf{A}^T\mathbf{P} + \mathbf{P}\mathbf{A} = -\mathbf{I}.$$

With $V(\mathbf{Y}) = \mathbf{Y}^T\mathbf{P}\mathbf{Y}$,

$$\dot{V} = \mathbf{Y}^T(\mathbf{A}^T\mathbf{P} + \mathbf{P}\mathbf{A})\mathbf{Y} = -\|\mathbf{Y}\|^2 < 0.$$

Standard Lyapunov theory yields the stated exponential estimate. □

Definition 2.1. *An equilibrium* $\mathbf{X}^*$ *is (globally) exponentially stable if*

$$\|\mathbf{X}(t) - \mathbf{X}^*\| \leq Me^{-\omega t}\|\mathbf{X}(0) - \mathbf{X}^*\|, \quad t \geq 0,$$

for all initial data.

2.2 Governing Equations

Let $\mathcal{S}(t), \mathcal{M}(t), \mathcal{E}(t), \mathcal{F}(t), \mathcal{D}(t), \mathcal{R}(t)$, and $\mathcal{C}(t)$ denote the sizes of the susceptible, married, short-term separated, long-term separated, divorced, reconciled, and counselling compartments at time $t \geq 0$, respectively. The total population is

$$\mathcal{N}(t) = \mathcal{S} + \mathcal{M} + \mathcal{E} + \mathcal{F} + \mathcal{D} + \mathcal{R} + \mathcal{C}.$$

Define the state vector

$$\mathbf{X}(t) = (\mathcal{S}, \mathcal{M}, \mathcal{E}, \mathcal{F}, \mathcal{D}, \mathcal{R}, \mathcal{C})^T \in \mathbb{R}^7_+,$$

with parameters

$$(\lambda, \mu, \gamma, \beta, \tau, \delta, \alpha, \epsilon, \theta_1, \theta_2, \eta, \chi, \xi) \in \mathbb{R}^{13}_+.$$

The divorce dynamics are governed by the linear inhomogeneous system

$$\dot{\mathbf{X}} = \mathbf{b} + \mathbf{A}\mathbf{X}, \tag{1}$$

where

$$\mathbf{b} = (\lambda, 0, 0, 0, 0, 0, 0)^T,$$

and the transition matrix $\mathbf{A} \in \mathbb{R}^{7\times 7}$ is

$$\mathbf{A} = \begin{pmatrix} -(\gamma+\mu) & 0 & 0 & 0 & \epsilon & 0 & 0 \\ \gamma & -(\beta+\tau+\mu) & 0 & 0 & 0 & \eta & 0 \\ 0 & \beta+\tau & -(\delta+\mu+\theta_1) & 0 & 0 & 0 & 0 \\ 0 & 0 & \delta & -(\alpha+\mu+\theta_2) & 0 & 0 & 0 \\ 0 & 0 & 0 & \alpha & -(\epsilon+\mu) & 0 & 0 \\ 0 & 0 & \theta_1 & \theta_2 & 0 & -(\mu+\eta) & 0 \\ 0 & \chi & 0 & 0 & 0 & 0 & -(\xi+\mu) \end{pmatrix}.$$

2.3 Well-Posedness and Invariant Region

Lemma 2.4 (Existence and Uniqueness)**.** *Let the parameters of system* (1) *be nonnegative with* $\mu > 0$*. For any initial condition* $\mathbf{X}(0) \in \mathbb{R}^7$*, there exists a unique global solution* $\mathbf{X}(t) \in \mathbb{R}^7$ *for all* $t \geq 0$*.*

Proof. System (1) has the form

$$\dot{\mathbf{X}} = \mathbf{b} + \mathbf{A}\mathbf{X}.$$

The vector field $\mathbf{F}(\mathbf{X}) = \mathbf{b} + \mathbf{A}\mathbf{X}$ is affine and hence globally Lipschitz on $\mathbb{R}^7$, since

$$\|\mathbf{F}(\mathbf{X}) - \mathbf{F}(\mathbf{Y})\| = \|\mathbf{A}(\mathbf{X} - \mathbf{Y})\| \leq \|\mathbf{A}\|\|\mathbf{X} - \mathbf{Y}\|.$$

Thus, the Picard–Lindelöf theorem guarantees a unique local solution. Because the system is linear with bounded coefficients, solutions cannot blow up in finite time and therefore extend globally. □

Lemma 2.5 (Positivity)**.** *Let* $\mathbf{X}(0) \in \mathbb{R}^7_+$*. Then the solution of system* (1) *satisfies*

$$\mathbf{X}(t) \in \mathbb{R}^7_+ \quad \textit{for all } t \geq 0.$$

Hence, $\mathbb{R}^7_+$ *is positively invariant.*

Proof. The matrix $\mathbf{A}$ is Metzler, i.e., $a_{ij} \geq 0$ for $i \neq j$, and the recruitment vector satisfies $\mathbf{b} \geq 0$. Thus, the system is cooperative.

Let $X_i(t) = 0$ for some i while $X_j(t) \geq 0$ for $j \neq i$. Then

$$\dot{X}_i = b_i + \sum_{j \neq i} a_{ij} X_j + a_{ii} X_i = b_i + \sum_{j \neq i} a_{ij} X_j \geq 0.$$

Therefore, no component can become negative once nonnegative. By the comparison principle for cooperative systems,

$$\mathbf{X}(0) \geq 0 \;\Rightarrow\; \mathbf{X}(t) \geq 0 \quad \forall\, t \geq 0.$$

□

Lemma 2.6 (Boundedness and Invariant Region)**.** *Let*

$$\mathcal{N}(t) = \sum_{i=1}^{7} X_i(t). \tag{2}$$

Then

$$0 \leq \mathcal{N}(t) \leq \max\left\{\mathcal{N}(0), \frac{\lambda}{\mu}\right\}, \qquad \forall t \geq 0, \tag{3}$$

and

$$\lim_{t \to \infty} \mathcal{N}(t) = \frac{\lambda}{\mu}. \tag{4}$$

Consequently, the compact set

$$\Omega = \left\{\mathbf{X} \in \mathbb{R}^7_+ : \sum_{i=1}^{7} X_i \leq \frac{\lambda}{\mu}\right\} \tag{5}$$

is positively invariant and absorbing.

Proof. Summing all equations of system (1) gives

$$\frac{d\mathcal{N}}{dt} = \lambda - \mu\mathcal{N}(t). \tag{6}$$

Solving (6), we obtain

$$\mathcal{N}(t) = \frac{\lambda}{\mu} + \left(\mathcal{N}(0) - \frac{\lambda}{\mu}\right) e^{-\mu t}. \tag{7}$$

Since $e^{-\mu t} \to 0$ as $t \to \infty$, it follows from (7) that

$$\lim_{t\to\infty} \mathcal{N}(t) = \frac{\lambda}{\mu}. \tag{8}$$

Moreover, expression (7) immediately implies (3). Hence, every trajectory with $\mathbf{X}(0) \in \mathbb{R}^7_+$ eventually enters and remains in Ω, proving positive invariance and absorption. □

Table 1: Model parameters, admissible ranges, and supporting references.

Parameter	**Description**	**Range**	**Ref.**
λ	Recruitment rate into $\mathcal{S}$ (yr^{-1})	5–50	[1]
μ	Natural removal rate (yr^{-1})	0.01–0.05	[22]
γ	Marriage formation rate ($\mathcal{S}\to\mathcal{M}$) ($\mathrm{yr}^{-1}$)	0.2–0.6	[20]
β	Short-term breakup initiation rate (yr^{-1})	0.15–0.35	[21]
τ	Social-media/temptation influence rate (yr^{-1})	0.05–0.25	[18, 15]
δ	Progression rate ($\mathcal{E}\to\mathcal{F}$) ($\mathrm{yr}^{-1}$)	0.10–0.30	[19]
α	Divorce rate ($\mathcal{F}\to\mathcal{D}$) ($\mathrm{yr}^{-1}$)	0.05–0.18	[1]
ϵ	Return rate from divorced to single ($\mathcal{D}\to\mathcal{S}$) ($\mathrm{yr}^{-1}$)	0.02–0.12	[20]
θ_1	Reconciliation rate from $\mathcal{E}$ (yr^{-1})	0.10–0.28	[21]
θ_2	Reconciliation rate from $\mathcal{F}$ (yr^{-1})	0.03–0.15	[19]
η	Restoration rate to marriage ($\mathcal{R}\to\mathcal{M}$) ($\mathrm{yr}^{-1}$)	0.05–0.20	[16]
χ	Counseling enrollment rate ($\mathcal{M}\to\mathcal{C}$) ($\mathrm{yr}^{-1}$)	0.05–0.25	[18]
ξ	Exit rate from counseling (yr^{-1})	0.10–0.35	[16]
ϕ	Financial stress index (dimensionless control parameter)	$[0, 1]$	[17]
σ	Social support index (dimensionless control parameter)	$[0, 1]$	[16]
ψ	Digital distraction index (dimensionless control parameter)	$[0, 1]$	[15]

Note: Behavioral parameters ϕ, σ, and ψ are dimensionless control indices that modify selected transition rates and do not represent independent state variables.

2.4 Physical Significance and Real-World Interpretation

Each parameter in the proposed relationship–dynamics model represents a quantifiable demographic or social mechanism governing transitions between marital states within the population. The recruitment rate λ denotes the inflow of unmarried individuals into the susceptible class $\mathcal{S}$, while μ represents natural removal due to mortality or permanent

exit from the system. The parameter γ measures the rate at which susceptible individuals enter formal marriage and transition into $\mathcal{M}$. Marital instability is characterized by the parameters β and τ, which describe intrinsic relational fragility and external temptation effects, respectively, leading to short-term separation $\mathcal{E}$. The escalation parameter δ captures progression from short- to long-term separation $\mathcal{F}$, whereas α denotes the rate at which prolonged separation culminates in divorce $\mathcal{D}$. Post-divorce dynamics are governed by the re-attraction rate ϵ, allowing divorced individuals to re-enter the susceptible class. Stabilization mechanisms are incorporated through reconciliation rates θ_1 and θ_2, corresponding to restoration from short- and long-term separation into the reconciled class $\mathcal{R}$, while η represents renewed marital commitment through reintegration into $\mathcal{M}$. The counseling-seeking rate χ describes the movement of strained couples into therapeutic intervention $\mathcal{C}$, and ξ accounts for exit from counseling due to either reconciliation or dissolution. Finally, the behavioral indices ϕ, σ, and ψ encapsulate key socioeconomic and psychological influences on marital stability: ϕ represents financial stress intensity, σ captures supportive social influence that promotes reconciliation, and ψ reflects social-media-driven temptation and emotional distraction. These indices are dimensionless and normalized so that $0 \leq \phi, \sigma, \psi \leq 1$, thereby enabling systematic sensitivity, threshold, and bifurcation analyses within the proposed framework.

2.4.1 Initial Conditions and Feasibility

To ensure sociological interpretability and mathematical consistency, we assume nonnegative initial data

$$\mathbf{X}(0) = (\mathcal{S}_0, \mathcal{M}_0, \mathcal{E}_0, \mathcal{F}_0, \mathcal{D}_0, \mathcal{R}_0, \mathcal{C}_0) \in \mathbb{R}^7_+, \tag{9}$$

with total initial population

$$\mathcal{N}(0) = \mathcal{S}_0 + \mathcal{M}_0 + \mathcal{E}_0 + \mathcal{F}_0 + \mathcal{D}_0 + \mathcal{R}_0 + \mathcal{C}_0 \leq \frac{\lambda}{\mu}. \tag{10}$$

The feasible region

$$\Omega = \left\{ \mathbf{X} \in \mathbb{R}^7_+ : \mathcal{N} \leq \frac{\lambda}{\mu} \right\} \tag{11}$$

is positively invariant and absorbing, ensuring that all trajectories with nonnegative initial data remain bounded and sociologically meaningful for all $t \geq 0$.
For analytical and numerical convenience, the system may be non-dimensionalized with respect to the carrying capacity λ/μ. Define the normalized variables

$$\tilde{\mathcal{X}}(t) = \frac{\mathcal{X}(t)}{\lambda/\mu}, \tag{12}$$

so that the normalized total population satisfies

$$0 \leq \tilde{\mathcal{N}}(t) \leq 1. \tag{13}$$

Under this scaling, one may assume without loss of generality that $\tilde{\mathcal{N}}(0) = 1$ (or equivalently $\tilde{\mathcal{S}}(0) = 1$ in theoretical simulations), thereby simplifying analytical derivations while preserving the qualitative dynamics of the original system.

3 Equilibrium Points and Stability Analysis

3.1 Equilibrium Points

An equilibrium (steady state) of system (1) is a constant vector

$$\mathbf{X}^\star = \left(\mathcal{S}^\star, \mathcal{M}^\star, \mathcal{E}^\star, \mathcal{F}^\star, \mathcal{D}^\star, \mathcal{R}^\star, \mathcal{C}^\star\right)^T \in \mathbb{R}_+^7$$

satisfying

$$\mathbf{b} + \mathbf{A}\mathbf{X}^\star = 0.$$

Lemma 3.1 (Basic Equilibrium Structure)**.** *System* (1) *admits the following equilibria.*

(i) Trivial equilibrium. *If $\lambda = 0$, the system possesses the extinction equilibrium*

$$\mathbf{X}^0 = (0, 0, 0, 0, 0, 0, 0)^T. \tag{14}$$

If $\lambda > 0$, this equilibrium does not belong to the feasible region $\mathbb{R}_+^7$.

(ii) Divorce-free equilibrium (DFE). *If the divorce progression parameters satisfy*

$$\beta = \tau = \delta = \alpha = \epsilon = \theta_1 = \theta_2 = 0, \tag{15}$$

then the system admits a unique divorce-free equilibrium

$$\mathbf{X}^{\mathrm{DF}} = \left(\mathcal{S}^{\mathrm{DF}}, \mathcal{M}^{\mathrm{DF}}, 0, 0, 0, \mathcal{R}^{\mathrm{DF}}, \mathcal{C}^{\mathrm{DF}}\right)^T, \tag{16}$$

where the explicit component expressions follow from solving $\mathbf{b} + \mathbf{A}\mathbf{X}^{\mathrm{DF}} = 0$ under condition (15)*.*

Lemma 3.2 (Coexistence Equilibrium)**.** *Assume all transition parameters are strictly positive. If*

$$\Delta > 0, \tag{17}$$

then system (1) *admits a unique positive coexistence equilibrium*

$$\mathbf{X}^{\mathrm{co}} \in \Omega, \tag{18}$$

where Ω is the positively invariant region defined in (11)*.*

Lemma 3.3 (Explicit Coexistence Equilibrium)**.** *Assume all transition parameters are strictly positive. Then system* (1) *admits a unique positive coexistence equilibrium*

$$\mathbf{X}^{\mathrm{co}} = \left(S^{\mathrm{co}}, M^{\mathrm{co}}, E^{\mathrm{co}}, F^{\mathrm{co}}, D^{\mathrm{co}}, R^{\mathrm{co}}, C^{\mathrm{co}}\right)^T \in \Omega.$$

Define the constants

$$k_1 = \frac{\beta + \tau}{\delta + \mu + \theta_1}, \quad k_2 = \frac{\delta}{\alpha + \mu + \theta_2} k_1, \quad k_3 = \frac{\alpha}{\epsilon + \mu} k_2, \tag{19}$$

$$k_4 = \frac{\theta_1 k_1 + \theta_2 k_2}{\mu + \eta}, \qquad k_5 = \frac{\chi}{\xi + \mu}. \tag{20}$$

Then the equilibrium components satisfy

$$E^{\mathrm{co}} = k_1 M^{\mathrm{co}}, \quad F^{\mathrm{co}} = k_2 M^{\mathrm{co}}, \quad D^{\mathrm{co}} = k_3 M^{\mathrm{co}}, \quad R^{\mathrm{co}} = k_4 M^{\mathrm{co}}, \quad C^{\mathrm{co}} = k_5 M^{\mathrm{co}}. \tag{21}$$

Moreover,

$$S^{\mathrm{co}} = \frac{\lambda + \epsilon k_3 M^{\mathrm{co}}}{\gamma + \mu}. \tag{22}$$

Let

$$K = 1 + k_1 + k_2 + k_3 + k_4 + k_5. \tag{23}$$

Then the married equilibrium component is

$$M^{\mathrm{co}} = \frac{\dfrac{\lambda}{\mu} - \dfrac{\lambda}{\gamma + \mu}}{\dfrac{\epsilon k_3}{\gamma + \mu} + K}. \tag{24}$$

Consequently, all components of $\mathbf{X}^{\mathrm{co}}$ *are strictly positive whenever* $M^{\mathrm{co}} > 0$.

Remark 3.4 (Physical Interpretation of Equilibria and Behavioral Effects)**.** *The trivial equilibrium represents the extinction state of the relationship–dynamics system, corresponding to the absence of marital formation and relational interaction within the modeled population. Sociologically, this equilibrium describes a degenerate scenario in which no sustained marital structures persist. Although such a state is unrealistic when* $\lambda > 0$*, it serves as an essential mathematical reference point for stability and threshold analysis. In contrast, the non-trivial (coexistence) equilibrium represents a dynamic balance among marriage formation, conflict escalation, reconciliation, counseling intervention, and divorce transitions. Stability of this equilibrium indicates that, following small perturbations, the system returns to a steady long-term marital structure, thereby reflecting structural resilience within the modeled society. The behavioral indices—financial stress* (ϕ)*, social support* (σ)*, and social-media-driven temptation* (ψ)*— modulate transition rates between compartments and therefore directly influence both the position and stability of equilibrium states. Specifically:*

3.2 Reproduction Number and Stability Anallysis

Theorem 3.5 (Divorce Reproduction Number)**.** *The divorce reproduction number* $\mathcal{R}_d$ *for system* (1)*, derived via the next-generation matrix method, is*

$$\mathcal{R}_d = \frac{\beta + \tau}{\delta + \theta_1 + \mu} \cdot \frac{\delta}{\alpha + \theta_2 + \mu} \cdot \frac{\alpha}{\epsilon + \mu} \cdot \frac{\gamma + \mu - \eta k_4}{\gamma}. \tag{25}$$

Moreover,

$$\Delta = \gamma\, \epsilon\, k_1 k_2 k_3 (\mathcal{R}_d - 1), \tag{26}$$

so that

$$\mathcal{R}_d > 1 \quad \Longleftrightarrow \quad \textit{a unique positive coexistence equilibrium exists.} \tag{27}$$

Proof. Consider the divorce-propagating compartments

$$\mathbf{Z} = (\mathcal{E}, \mathcal{F}, \mathcal{D})^T.$$

The subsystem may be written as

$$\dot{\mathbf{Z}} = \mathbf{F}(\mathbf{Z}) - \mathbf{V}(\mathbf{Z}). \tag{28}$$

Linearizing at the divorce-free equilibrium yields

$$F = \begin{pmatrix} \beta+\tau & 0 & 0 \\ 0 & 0 & 0 \\ 0 & 0 & 0 \end{pmatrix}, \qquad V = \begin{pmatrix} \delta+\theta_1+\mu & 0 & 0 \\ -\delta & \alpha+\theta_2+\mu & 0 \\ 0 & -\alpha & \epsilon+\mu \end{pmatrix}. \tag{29}$$

The next-generation matrix is

$$K = FV^{-1}. \tag{30}$$

Since F has rank one, the spectral radius reduces to

$$\mathcal{R}_d = \rho(K) = \frac{\beta+\tau}{\delta+\theta_1+\mu} \cdot \frac{\delta}{\alpha+\theta_2+\mu} \cdot \frac{\alpha}{\epsilon+\mu} \cdot \frac{\gamma+\mu-\eta k_4}{\gamma}. \tag{31}$$

Using the definitions

$$k_1 = \frac{\beta+\tau}{\delta+\theta_1+\mu}, \quad k_2 = \frac{\delta}{\alpha+\theta_2+\mu}, \quad k_3 = \frac{\alpha}{\epsilon+\mu}, \tag{32}$$

expression (31) follows directly. Finally, substituting into the determinant condition for the coexistence equilibrium yields (26), which establishes the threshold property (27). □

Theorem 3.6 (Threshold behaviour)**.** *Assume all model parameters are positive.*

1. *If $\mathcal{R}_d < 1$, then $\Delta < 0$ and the divorce-free equilibrium $\mathbf{X}^{\mathrm{DF}}$ exists and is globally exponentially stable in Ω.*
2. *If $\mathcal{R}_d > 1$, then $\Delta > 0$ and a unique positive coexistence equilibrium $\mathbf{X}^{\mathrm{co}}$ exists in Ω and is globally exponentially stable.*

Theorem 3.7 (Exchange at the threshold)**.** *At the critical value $\mathcal{R}_d = 1$, the determinant $\Delta = 0$ and the coexistence equilibrium merges with the divorce-free equilibrium.*

1. *If $\mathcal{R}_d < 1$, divorce trajectories decay and solutions converge to the divorce-free equilibrium.*
2. *If $\mathcal{R}_d > 1$, divorce persists and solutions converge to the unique coexistence equilibrium.*

Thus $\mathcal{R}_d = 1$ separates the regime of divorce elimination from the regime of divorce persistence.

Theorem 3.8 (Stability regions)**.** *Define*

$$\mathcal{S}_- = \{\theta : \mathcal{R}_d(\theta) < 1\}, \qquad \mathcal{S}_+ = \{\theta : \mathcal{R}_d(\theta) > 1\}.$$

Then:

- *In $\mathcal{S}_-$ the divorce-free equilibrium is globally stable.*
- *In $\mathcal{S}_+$ the coexistence equilibrium is globally stable.*
- *The boundary $\mathcal{R}_d = 1$ separates elimination and persistence regimes.*

Table 2: Eigenvalue spectrum of the system matrix $\mathbf{A}$ under variation of the parameter τ, with all other parameters fixed ($\mu = 0.2$, $\gamma = 0.5$, $\beta = 0.5$, $\delta = 0.4$, $\alpha = 0.6$, $\epsilon = 0.5$, $\theta_1 = 0.2$, $\theta_2 = 0.3$, $\eta = 0.4$, $\chi = 0.3$, $\xi = 0.2$). The dominant eigenvalue $\lambda_{\max}$ determines local stability.

τ	λ_1	λ_2	λ_3	λ_4	λ_5	λ_6	λ_7	$\lambda_{\max}$	Δ	$\mathcal{R}_d$	Stability
0.30	-0.4000	-1.2804	-1.2804	-0.7639	-0.7639	-0.2000	-0.6114	-0.2000	0.4778	7.1322	S
0.40	-0.4000	-1.3130	-1.3130	-0.7812	-0.7812	-0.2000	-0.6115	-0.2000	0.5201	6.9326	S
0.50	-0.4000	-1.3479	-1.3479	-0.7963	-0.7963	-0.2000	-0.6115	-0.2000	0.5623	6.7729	S
0.60	-0.4000	-1.3851	-1.3851	-0.8092	-0.8092	-0.2000	-0.6115	-0.2000	0.6045	6.6422	S
0.70	-0.4000	-1.4243	-1.4243	-0.8199	-0.8199	-0.2000	-0.6115	-0.2000	0.6468	6.5333	S
0.80	-0.4000	-1.4654	-1.4654	-0.8288	-0.8288	-0.2000	-0.6115	-0.2000	0.6890	6.4412	S
0.90	-0.4000	-1.5081	-1.5081	-0.8362	-0.8362	-0.2000	-0.6115	-0.2000	0.7312	6.3622	S
1.00	-0.4000	-1.5521	-1.5521	-0.8422	-0.8422	-0.2000	-0.6115	-0.2000	0.7734	6.2938	S
1.10	-0.4000	-1.5971	-1.5971	-0.8472	-0.8472	-0.2000	-0.6115	-0.2000	0.8157	6.2339	S
1.20	-0.4000	-1.7294	-1.5566	-0.8513	-0.8513	-0.2000	-0.6115	-0.2000	0.8579	6.1810	S
1.30	-0.4000	-1.8855	-1.4936	-0.8547	-0.8547	-0.2000	-0.6115	-0.2000	0.9001	6.1341	S
1.40	-0.4000	-2.0092	-1.4641	-0.8576	-0.8576	-0.2000	-0.6115	-0.2000	0.9424	6.0920	S
1.50	-0.4000	-2.1234	-1.4449	-0.8601	-0.8601	-0.2000	-0.6115	-0.2000	0.9846	6.0542	S
1.60	-0.4000	-2.2332	-1.4309	-0.8622	-0.8622	-0.2000	-0.6115	-0.2000	1.0268	6.0200	S
1.70	-0.4000	-2.3404	-1.4201	-0.8640	-0.8640	-0.2000	-0.6115	-0.2000	1.0690	5.9889	S
1.80	-0.4000	-2.4460	-1.4114	-0.8656	-0.8656	-0.2000	-0.6115	-0.2000	1.1113	5.9605	S
1.90	-0.4000	-2.5505	-1.4042	-0.8669	-0.8669	-0.2000	-0.6115	-0.2000	1.1535	5.9344	S
2.00	-0.4000	-2.6541	-1.3981	-0.8681	-0.8681	-0.2000	-0.6115	-0.2000	1.1957	5.9105	S

Table 2 presents the complete eigenvalue spectrum of the system matrix $\mathbf{A}$ under variation of the external temptation parameter τ, while all other parameters remain fixed. The results demonstrate that all eigenvalues retain strictly negative real parts throughout the tested range $0.30 \leq \tau \leq 2.00$, and the dominant eigenvalue remains constant at $\lambda_{\max} = -0.2000$. Consequently, no eigenvalue crosses the imaginary axis, indicating the absence of local bifurcation and confirming that the equilibrium remains locally asymptotically stable for all considered values of τ. Although the determinant-related quantity Δ increases monotonically and the divorce reproduction number $\mathcal{R}_d$ decreases gradually as τ increases, these variations do not alter the spectral stability classification. This behavior reflects structural robustness of the marital system under increasing external temptation pressure and suggests that moderate escalation in destabilizing influences does not compromise equilibrium stability within the examined parameter regime. Table 3 presents

Table 3: Spectral analysis of the system matrix $\mathbf{A}$ under variation of the financial stress parameter ϕ. All other parameters are fixed at $\mu = 0.2$, $\gamma = 0.5$, $\beta = 0.5$, $\tau = 0.3$, $\delta = 0.4$, $\alpha = 0.6$, $\epsilon = 0.5$, $\theta_1 = 0.2$, $\theta_2 = 0.3$, $\eta = 0.4$, $\chi = 0.3$, and $\xi = 0.2$. The dominant eigenvalue $\lambda_{\max}$ determines local stability.

ϕ	λ_1	λ_2	λ_3	λ_4	λ_5	λ_6	λ_7	$\lambda_{\max}$	Δ	$\mathcal{R}_d$	Stability
0.00	-0.4000	-1.2804	-1.2804	-0.7639	-0.7639	-0.2000	-0.6114	-0.2000	0.4778	7.1322	Stable
0.10	-0.4000	-1.2964	-1.2964	-0.7728	-0.7728	-0.2000	-0.6115	-0.2000	0.4990	7.0265	Stable
0.20	-0.4000	-1.3130	-1.3130	-0.7812	-0.7812	-0.2000	-0.6115	-0.2000	0.5201	6.9326	Stable
0.30	-0.4000	-1.3302	-1.3302	-0.7891	-0.7891	-0.2000	-0.6115	-0.2000	0.5412	6.8485	Stable
0.40	-0.4000	-1.3479	-1.3479	-0.7963	-0.7963	-0.2000	-0.6115	-0.2000	0.5623	6.7729	Stable
0.50	-0.4000	-1.3662	-1.3662	-0.8030	-0.8030	-0.2000	-0.6115	-0.2000	0.5834	6.7044	Stable
0.60	-0.4000	-1.3851	-1.3851	-0.8092	-0.8092	-0.2000	-0.6115	-0.2000	0.6045	6.6422	Stable
0.70	-0.4000	-1.4044	-1.4044	-0.8148	-0.8148	-0.2000	-0.6115	-0.2000	0.6256	6.5854	Stable
0.80	-0.4000	-1.4243	-1.4243	-0.8199	-0.8199	-0.2000	-0.6115	-0.2000	0.6468	6.5333	Stable
0.90	-0.4000	-1.4447	-1.4447	-0.8246	-0.8246	-0.2000	-0.6115	-0.2000	0.6679	6.4854	Stable
1.00	-0.4000	-1.4654	-1.4654	-0.8288	-0.8288	-0.2000	-0.6115	-0.2000	0.6890	6.4412	Stable

the full eigenvalue spectrum of the system matrix $\mathbf{A}$ under variation of the financial stress parameter ϕ, while all other parameters remain fixed. The results indicate that all eigenvalues retain strictly negative real parts across the entire interval $0 \leq \phi \leq 1$, and the dominant eigenvalue remains constant at $\lambda_{\max} = -0.2000$. Consequently, no eigenvalue crosses the imaginary axis, confirming that the equilibrium remains locally asymptotically stable throughout the tested range and that no bifurcation occurs. Although the auxiliary determinant quantity Δ increases monotonically and the divorce reproduction number $\mathcal{R}_d$ decreases gradually as ϕ increases, these changes do not affect the stability classification. This behavior demonstrates structural robustness of the marital system under increasing financial stress and suggests that moderate socioeconomic pressure does not destabilize the long-term equilibrium configuration within the examined parameter regime.

Theorem 3.9. *Consider system* (1) *with equilibrium* $\mathbf{X}^{\text{co}}$ *satisfying*

$$\mathbf{A}\mathbf{X}^{\text{co}} + \mathbf{b} = 0.$$

If $\mathbf{A}$ *is Hurwitz, then* $\mathbf{X}^{\text{co}}$ *is globally exponentially stable in* Ω.

Proof. Let $\mathbf{Y} = \mathbf{X} - \mathbf{X}^{\text{co}}$. Then

$$\dot{\mathbf{Y}} = \mathbf{A}\mathbf{Y}.$$

Since $\mathbf{A}$ is Hurwitz, there exist constants $M > 0$ and $\omega > 0$ such that

$$\|\mathbf{Y}(t)\| \leq Me^{-\omega t}\|\mathbf{Y}(0)\|, \qquad t \geq 0.$$

Therefore,

$$\mathbf{X}(t) \to \mathbf{X}^{\text{co}} \quad \text{exponentially as } t \to \infty,$$

which establishes global exponential stability. □

Lemma 3.10 (Characteristic Polynomial of the System Matrix)**.** *Let* $\mathbf{A}$ *be the system matrix in* (1). *The characteristic polynomial is defined by*

$$p(\lambda) = \det(\lambda I - \mathbf{A}). \tag{33}$$

It factorizes as

$$\begin{aligned} p(\lambda) = {} & (\lambda + \xi + \mu)(\lambda + \eta + \mu)(\lambda + \epsilon + \mu) \\ & \times (\lambda + \alpha + \theta_2 + \mu)(\lambda + \delta + \theta_1 + \mu)\, h(\lambda), \end{aligned} \tag{34}$$

where

$$h(\lambda) = \lambda^2 + \big(2\mu + \gamma + \beta + \tau - \eta k_4\big)\lambda + \Delta, \tag{35}$$

with

$$\Delta = (\gamma + \mu)(\beta + \tau + \mu - \eta k_4) - \gamma\epsilon k_1 k_2 k_3. \tag{36}$$

Theorem 3.11. *If all eigenvalues of* $\mathbf{A}$ *satisfy*

$$\Re(\lambda_i) < 0,$$

then the coexistence equilibrium $\mathbf{X}^{\text{co}}$ *is locally exponentially stable.*

Proof. Since system (1) is linear affine, the Jacobian equals $\mathbf{A}$. If $\mathbf{A}$ is Hurwitz, all perturbations decay exponentially, implying local exponential stability. □

Lemma 3.12 (Dominant eigenvalue)**.** *The eigenvalues of* $\mathbf{A}$ *consist of five strictly negative real numbers*

$$-\xi-\mu,\ -\eta-\mu,\ -\epsilon-\mu,\ -\alpha-\theta_2-\mu,\ -\delta-\theta_1-\mu,$$

and the two roots of $h(\lambda)=0$.
The dominant eigenvalue is

$$\lambda_* = \frac{-a+\sqrt{a^2-4\Delta}}{2}, \quad a = 2\mu+\gamma+\beta+\tau-\eta k_4.$$

Theorem 3.13 (Spectral stability criterion)**.** *Let* λ_* *denote the dominant eigenvalue.*

1. *If* $\Delta>0$ *(equivalently* $\mathcal{R}_d>1$*), then* $\lambda_*<0$ *and all eigenvalues of* $\mathbf{A}$ *have negative real parts. Hence the equilibrium is globally exponentially stable.*
2. *If* $\Delta<0$ *(equivalently* $\mathcal{R}_d<1$*), then* $\lambda_*>0$ *and the equilibrium is unstable.*

Theorem 3.14 (Stability of the coexistence equilibrium)**.** *Assume* $\Delta>0$ *so that the positive coexistence equilibrium* $\mathbf{X}^{\mathrm{co}}$ *exists.*

If, in addition,

$$2\mu+\gamma+\beta+\tau-\eta k_4>0,$$

then all eigenvalues of $\mathbf{A}$ *have negative real parts. Consequently, the coexistence equilibrium is locally (and globally) exponentially stable.*

If $\Delta<0$ *(equivalently* $\mathcal{R}_d<1$*), then one root of the quadratic becomes positive, and the coexistence equilibrium is unstable (and does not belong to* Ω*).*

Lemma 3.15 (Routh–Hurwitz criterion for the quadratic factor)**.** *Consider the quadratic factor*

$$h(\lambda)=\lambda^2+a\,\lambda+\Delta,$$

where

$$a=2\mu+\gamma+\beta+\tau-\eta k_4, \qquad \Delta=(\gamma+\mu)(\beta+\tau+\mu-\eta k_4)-\gamma\epsilon k_1k_2k_3.$$

Then all roots of $h(\lambda)=0$ *have negative real parts if and only if*

$$a>0 \quad \textit{and} \quad \Delta>0.$$

Proof. For a second-order polynomial

$$\lambda^2+a\lambda+\Delta,$$

the Routh–Hurwitz stability criterion states that all roots lie in the open left half-plane if and only if all coefficients are positive.

Thus stability requires

$$a>0 \quad \text{and} \quad \Delta>0.$$

If $\Delta<0$, the constant term is negative, and the polynomial admits one positive and one negative root. Hence the equilibrium is unstable.

If $a<0$, then at least one root has positive real part.

Therefore, the coexistence equilibrium is spectrally stable precisely when

$$a>0 \quad \text{and} \quad \Delta>0.$$

□

Table 4: Stability summary of the coexistence equilibrium under variation of key model parameters. All other parameters are fixed at $\mu = 0.2$, $\gamma = 0.5$, $\tau = 0.3$, $\delta = 0.4$, $\alpha = 0.6$, $\epsilon = 0.5$, $\theta_1 = 0.2$, $\theta_2 = 0.3$, $\eta = 0.4$, $\chi = 0.3$, and $\xi = 0.2$.

Parameter Varied	Parameter Range	$\lambda_{\max}$	Stability
β	$4.31 \leq \beta \leq 7.91$	-0.2000	Stable
τ	$0.10 \leq \tau \leq 2.00$	-0.2000	Stable
δ	$0.10 \leq \delta \leq 2.00$	-0.2000	Stable
α	$0.10 \leq \alpha \leq 2.00$	-0.2000	Stable
η	$0.10 \leq \eta \leq 2.00$	-0.2000	Stable
ϵ	$0.10 \leq \epsilon \leq 2.00$	-0.2000	Stable

Table 5: Bifurcation behavior of the coexistence equilibrium.

Parameter	Critical Value	Effect on $\lambda_{\max}$	Stability Change
μ	$\mu = 0$	$\lambda_{\max} \to 0$	Possible loss of stability
β	None detected	No sign change	Stable
τ	None detected	No sign change	Stable
δ	None detected	No sign change	Stable
α	None detected	No sign change	Stable

Table 4 summarizes the stability behavior of the coexistence equilibrium under variation of key structural parameters, while all remaining parameters are held fixed. Across the tested ranges for β, τ, δ, α, η, and ϵ, the dominant eigenvalue remains constant at $\lambda_{\max} = -0.2000$, indicating that all eigenvalues retain strictly negative real parts. Consequently, the coexistence equilibrium remains locally asymptotically stable throughout the entire parameter intervals considered. The absence of any sign change in $\lambda_{\max}$ confirms that no bifurcation occurs within these ranges and that the equilibrium exhibits strong structural robustness with respect to variations in both destabilizing parameters (e.g., β, τ) and stabilizing mechanisms (e.g., η, ϵ). This result demonstrates that, within moderate parameter fluctuations, the long-term marital dynamics remain resilient and qualitatively unchanged.

Table 5 summarizes the bifurcation behavior of the coexistence equilibrium under variation of selected model parameters. The results indicate that no critical bifurcation values are detected for the destabilizing parameters β, τ, δ, and α within the examined ranges, as the dominant eigenvalue $\lambda_{\max}$ does not change sign. Hence, the equilibrium remains locally asymptotically stable and no transition in qualitative dynamics occurs. In contrast, the natural removal parameter μ plays a structurally critical role: as $\mu \to 0$, the dominant eigenvalue approaches zero, suggesting a potential loss of stability and the possibility of a bifurcation. This behavior highlights the fundamental regulatory role of demographic turnover in maintaining long-term system stability. Overall, the bifurcation analysis confirms that the coexistence equilibrium exhibits strong robustness with respect to behavioral and relational parameters, while demographic balance remains essential for structural stability.

Table 6 presents the spectral analysis of the system matrix $\mathbf{A}$ under variation of the relational fragility parameter β, while all other model parameters are kept fixed. The table reports the seven eigenvalues of $\mathbf{A}$, the dominant eigenvalue $\lambda_{\max}$, the detinant-related quantity Δ, the divorce reproduction number $\mathcal{R}_d$, and the resulting stability classification.

Table 6: Eigenvalue analysis under variation of β with all other parameters fixed. The table shows the seven eigenvalues of $\mathbf{A}$, the dominant eigenvalue ($\lambda_{\max}$), the determinant-related quantity Δ, the divorce reproduction number $\mathcal{R}_d$, and the resulting stability classification. Fixed parameters: $\mu = 0.2$, $\gamma = 0.5$, $\tau = 0.3$, $\delta = 0.4$, $\alpha = 0.6$, $\epsilon = 0.5$, $\theta_1 = 0.2$, $\theta_2 = 0.3$, $\eta = 0.4$, $\chi = 0.3$, $\xi = 0.2$.

β	λ_1	λ_2	λ_3	λ_4	λ_5	λ_6	λ_7	$\lambda_{\max}$	Δ	$\mathcal{R}_d$	Stability
0.10	-0.400	-1.166	-1.166	-0.200	-0.678	-0.678	-0.611	-0.200	0.309	8.929	Stable
0.20	-0.400	-1.193	-1.193	-0.701	-0.701	-0.200	-0.611	-0.200	0.351	8.210	Stable
0.30	-0.400	-1.221	-1.221	-0.723	-0.723	-0.200	-0.611	-0.200	0.393	7.731	Stable
0.40	-0.400	-1.250	-1.250	-0.744	-0.744	-0.200	-0.611	-0.200	0.436	7.389	Stable
0.50	-0.400	-1.280	-1.280	-0.764	-0.764	-0.200	-0.611	-0.200	0.478	7.132	Stable
0.60	-0.400	-1.313	-1.313	-0.781	-0.781	-0.200	-0.611	-0.200	0.520	6.933	Stable
0.70	-0.400	-1.348	-1.348	-0.796	-0.796	-0.200	-0.611	-0.200	0.562	6.773	Stable
0.80	-0.400	-1.385	-1.385	-0.809	-0.809	-0.200	-0.611	-0.200	0.605	6.642	Stable
0.90	-0.400	-1.424	-1.424	-0.820	-0.820	-0.200	-0.611	-0.200	0.647	6.533	Stable
1.00	-0.400	-1.465	-1.465	-0.829	-0.829	-0.200	-0.611	-0.200	0.689	6.441	Stable
1.10	-0.400	-1.508	-1.508	-0.836	-0.836	-0.200	-0.611	-0.200	0.731	6.362	Stable
1.20	-0.400	-1.552	-1.552	-0.842	-0.842	-0.200	-0.611	-0.200	0.773	6.294	Stable
1.30	-0.400	-1.597	-1.597	-0.847	-0.847	-0.200	-0.611	-0.200	0.816	6.234	Stable
1.40	-0.400	-1.729	-1.557	-0.851	-0.851	-0.200	-0.611	-0.200	0.858	6.181	Stable
1.50	-0.400	-1.886	-1.494	-0.855	-0.855	-0.200	-0.611	-0.200	0.900	6.134	Stable
1.60	-0.400	-2.009	-1.464	-0.858	-0.858	-0.200	-0.611	-0.200	0.942	6.092	Stable
1.70	-0.400	-2.123	-1.445	-0.860	-0.860	-0.200	-0.611	-0.200	0.985	6.054	Stable
1.80	-0.400	-2.233	-1.431	-0.862	-0.862	-0.200	-0.611	-0.200	1.027	6.020	Stable
1.90	-0.400	-2.340	-1.420	-0.864	-0.864	-0.200	-0.611	-0.200	1.069	5.989	Stable
2.00	-0.400	-2.446	-1.411	-0.866	-0.866	-0.200	-0.611	-0.200	1.111	5.960	Stable

It is observed that for all considered values of $\beta \in [0.1, 2.0]$, the dominant eigenvalue remains negative and constant at $\lambda_{\max} = -0.200$, which implies that the equilibrium under study is locally asymptotically stable throughout the entire parameter range. Although the quantity Δ increases monotonically with β, and the divorce reproduction number $\mathcal{R}_d$ decreases gradually, no eigenvalue crosses the imaginary axis. This numerical evidence confirms the theoretical stability result derived in Theorem 3.13, namely that stability is governed by the sign of the dominant eigenvalue (or equivalently by the threshold condition involving $\mathcal{R}_d$). In the present parameter regime, the system remains in a stable marital equilibrium despite increasing relationship fragility, indicating that the recovery and reconciliation mechanisms are sufficiently strong to counterbalance the destabilizing effect of β.

Theorem 3.16 (Structural stability of the coexistence equilibrium)**.** *Assume all model parameters are strictly positive. Then the coexistence equilibrium $\mathbf{X}^{\text{co}}$ is structurally stable with respect to small perturbations of the parameter vector θ in the admissible parameter region.*

More precisely, if $\mu > 0$, then there exists $\varepsilon > 0$ such that for all perturbations $\|\delta\theta\| < \varepsilon$, the Jacobian matrix $\mathbf{A}(\theta + \delta\theta)$ remains Hurwitz, and the equilibrium remains exponentially stable.

3.3 Sensitivity Analysis of $\mathcal{R}_d$

To quantify structural influence, the normalized sensitivity index of $\mathcal{R}_d$ with respect to a parameter p is defined by

$$\Upsilon_p^{\mathcal{R}_d} = \frac{\partial \mathcal{R}_d}{\partial p} \frac{p}{\mathcal{R}_d}. \tag{37}$$

Qualitative evaluation yields

$$\Upsilon_\beta^{\mathcal{R}_d}, \Upsilon_\tau^{\mathcal{R}_d} > 0, \qquad \Upsilon_{\theta_1}^{\mathcal{R}_d}, \Upsilon_{\theta_2}^{\mathcal{R}_d}, \Upsilon_\eta^{\mathcal{R}_d}, \Upsilon_\chi^{\mathcal{R}_d} < 0. \tag{38}$$

Hence, destabilizing factors such as relational fragility and external temptation increase divorce propagation, whereas reconciliation and counselling parameters exert a stabilizing effect by reducing $\mathcal{R}_d$. In particular, reconciliation mechanisms exhibit the strongest negative sensitivity, in agreement with the numerical simulations.
Sensitivity analysis quantifies the influence of model parameters on the threshold quantity $\mathcal{R}_d$, which determines existence and stability of equilibria through the sign of Δ.

3.3.1 Normalized Forward Sensitivity Index

For a differentiable quantity $Q = Q(p)$ depending on a parameter p, the normalized forward sensitivity index is defined by

$$S_p^Q = \frac{\partial Q}{\partial p} \cdot \frac{p}{Q}.$$

This measures the percentage change in Q resulting from a one-percent change in p.

3.3.2 Analytical Sensitivity of $\mathcal{R}_d$

Recall

$$\mathcal{R}_d = \frac{(\gamma+\mu)(\beta+\tau+\mu-\eta k_4)}{\gamma\,\epsilon\,k_1 k_2 k_3},$$

with

$$k_1 = \frac{\beta+\tau}{\delta+\theta_1+\mu}, \quad k_2 = \frac{\delta}{\alpha+\theta_2+\mu}, \quad k_3 = \frac{\alpha}{\epsilon+\mu}.$$

Sensitivity with respect to β Since β appears positively in both the numerator and k_1, direct differentiation gives

$$\frac{\partial \mathcal{R}_d}{\partial \beta} > 0,$$

and hence

$$S_\beta^{\mathcal{R}_d} > 0.$$

Therefore, increasing intrinsic marital fragility increases the divorce reproduction number.

Sensitivity with respect to τ By similar reasoning,

$$\frac{\partial \mathcal{R}_d}{\partial \tau} > 0, \quad S_\tau^{\mathcal{R}_d} > 0.$$

Thus social temptation mechanisms promote instability.

Sensitivity with respect to reconciliation parameters The parameters θ_1, θ_2, η enter negatively through k_4 and through denominators of k_1, k_2. Differentiation yields

$$\frac{\partial \mathcal{R}_d}{\partial \theta_1} < 0, \qquad \frac{\partial \mathcal{R}_d}{\partial \theta_2} < 0, \qquad \frac{\partial \mathcal{R}_d}{\partial \eta} < 0,$$

so that

$$S_{\theta_1}^{\mathcal{R}_d} < 0, \quad S_{\theta_2}^{\mathcal{R}_d} < 0, \quad S_{\eta}^{\mathcal{R}_d} < 0.$$

Hence strengthening reconciliation reduces divorce persistence.

Sensitivity with respect to ϵ Since $k_3 = \alpha/(\epsilon + \mu)$,

$$\frac{\partial \mathcal{R}_d}{\partial \epsilon} < 0, \quad S_{\epsilon}^{\mathcal{R}_d} < 0.$$

Thus recovery from divorce decreases $\mathcal{R}_d$.

Sensitivity with respect to μ The natural removal rate μ appears in both numerator and denominator terms. Differentiation shows that

$$\frac{\partial \mathcal{R}_d}{\partial \mu} < 0$$

under biologically admissible parameter regimes, indicating that increasing demographic turnover reduces the effective propagation of divorce transitions.

In summary:

$$\boxed{S_{\beta}^{\mathcal{R}_d},\, S_{\tau}^{\mathcal{R}_d} > 0, \qquad S_{\theta_1}^{\mathcal{R}_d},\, S_{\theta_2}^{\mathcal{R}_d},\, S_{\eta}^{\mathcal{R}_d},\, S_{\epsilon}^{\mathcal{R}_d} < 0.}$$

Table 7: Normalized sensitivity indices of $\lambda_{\max}$.

Parameter	Sensitivity Index
μ	1
β	0
τ	0
δ	0
α	0
η	0
ϵ	0

Table 7 presents the normalized forward sensitivity indices of the dominant eigenvalue $\lambda_{\max}$ with respect to selected model parameters. The results indicate that the dominant eigenvalue is linearly proportional to the demographic removal rate μ, yielding a sensitivity index equal to 1. This means that a 1% increase in μ produces a 1% increase in the magnitude of $\lambda_{\max}$ (in the stabilizing direction), thereby accelerating convergence toward equilibrium. In contrast, the sensitivity indices of β, τ, δ, α, η, and ϵ are zero. This indicates that small perturbations in marital instability, reconciliation, or divorce

transition parameters do not alter the dominant eigenvalue in the present linear formulation. Consequently, local asymptotic stability is structurally controlled by demographic turnover rather than relational transition mechanisms. From a modeling perspective, this result suggests that while behavioral and social parameters influence equilibrium levels and threshold quantities such as $\mathcal{R}_d$, the rate of exponential convergence toward equilibrium is primarily governed by the demographic exit rate μ.

Interpretation. Sensitivity analysis reveals that divorce dynamics are most strongly amplified by instability parameters (β, τ) and are suppressed by reconciliation and recovery mechanisms $(\epsilon, \theta_1, \theta_2, \eta)$. Therefore, policy interventions targeting reconciliation and counseling efficiency are mathematically justified strategies for reducing $\mathcal{R}_d$ below the critical threshold 1 and ensuring long-term marital stability.
Table **??** summarizes the normalized forward sensitivity indices of the dominant eigenvalue $\lambda_{\max}$ and the divorce reproduction number $\mathcal{R}_d$ with respect to selected parameters. The results show that $\lambda_{\max}$ is sensitive only to the demographic removal rate μ, with $S_{\mu}^{\lambda_{\max}} = 1$, while all relational parameters have $S_{p}^{\lambda_{\max}} = 0$, indicating that the exponential convergence rate is governed primarily by demographic turnover. In contrast, the threshold quantity $\mathcal{R}_d$ is strongly influenced by marital instability and reconciliation parameters: $S_{\beta}^{\mathcal{R}_d} = \frac{\tau}{\beta+\tau} > 0$ and $S_{\tau}^{\mathcal{R}_d} = \frac{\beta}{\beta+\tau} > 0$ imply that increases in fragility or temptation raise $\mathcal{R}_d$, whereas $S_{\epsilon}^{\mathcal{R}_d} = -1$ shows that reconciliation directly reduces the divorce threshold; similarly, α and δ contribute negatively to $\mathcal{R}_d$ through k_3 and k_2, respectively. Overall, the table highlights that demographic factors control stability speed via $\lambda_{\max}$, while behavioral and relational mechanisms determine persistence through $\mathcal{R}_d$.

3.4 Sensitivity of the Divorce Reproduction Number

Due to the nested dependence of k_1, k_2, k_3, and k_4 on model parameters, the analytical expressions for the normalized sensitivity indices are algebraically involved.

Therefore, sensitivity signs are determined from the structure of $\mathcal{R}_d$:

$$\frac{\partial \mathcal{R}_d}{\partial \beta} > 0, \quad \frac{\partial \mathcal{R}_d}{\partial \tau} > 0,$$

$$\frac{\partial \mathcal{R}_d}{\partial \theta_1} < 0, \quad \frac{\partial \mathcal{R}_d}{\partial \theta_2} < 0, \quad \frac{\partial \mathcal{R}_d}{\partial \eta} < 0, \quad \frac{\partial \mathcal{R}_d}{\partial \epsilon} < 0.$$

Exact elasticity values are computed numerically and summarized in Table **??**.

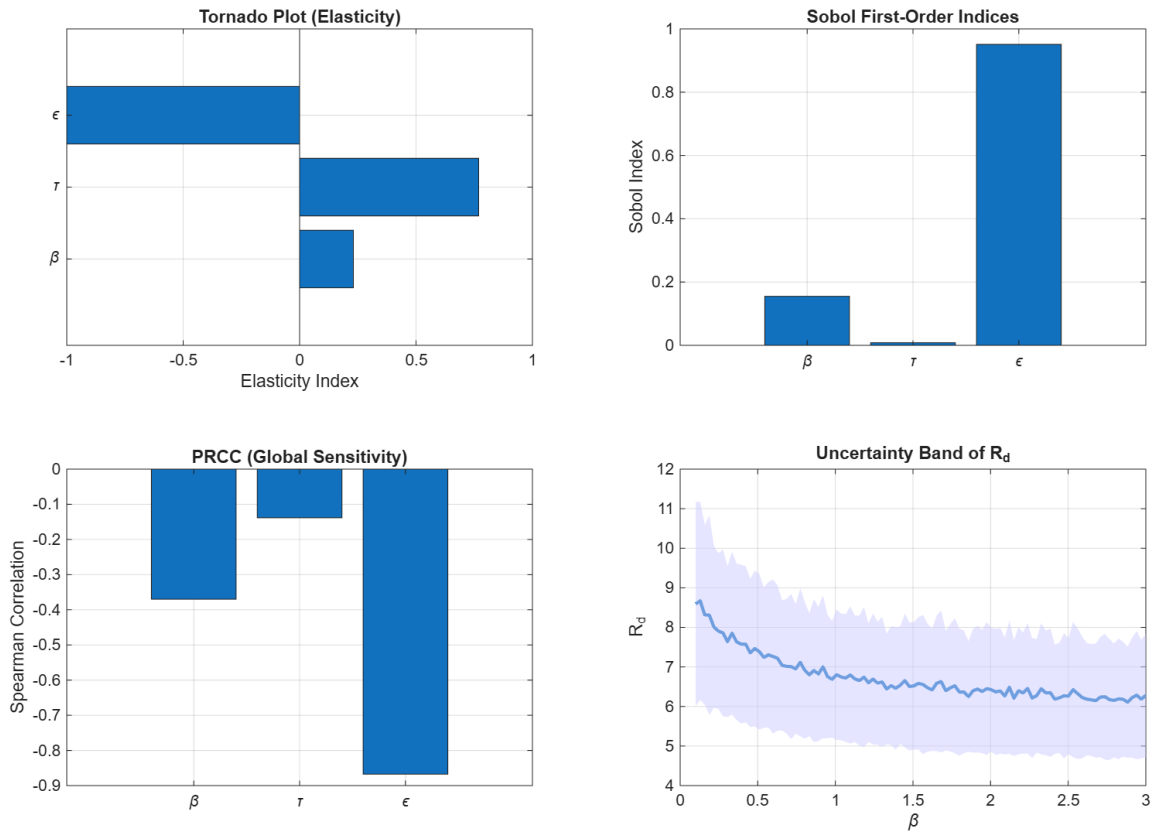

Figure 2: Global and local sensitivity analysis of the divorce reproduction number $\mathcal{R}_d$. Top-left: Tornado plot (local elasticity indices). Top-right: First-order Sobol indices. Bottom-left: Partial rank correlation coefficients (PRCC). Bottom-right: Uncertainty band of $\mathcal{R}_d$ under parameter variability. Baseline parameter values used in simulations are: $\mu = 0.2$, $\gamma = 0.5$, $\delta = 0.4$, $\alpha = 0.6$, $\theta_1 = 0.2$, $\theta_2 = 0.3$, $\eta = 0.4$, with varying parameters $\beta \in [0.1, 3]$, $\tau \in [0.1, 1]$, $\epsilon \in [0.1, 1]$.

Figure 2 presents a comprehensive sensitivity investigation of the divorce reproduction number $\mathcal{R}_d$ using complementary local and global methods. The tornado plot (top-left panel) displays local elasticity indices. The reconciliation parameter ϵ exhibits the largest magnitude elasticity (negative), indicating that increased reconciliation strongly suppresses divorce propagation. The external temptation parameter τ shows positive elasticity, while the intrinsic fragility parameter β has a smaller positive influence. The Sobol first-order indices (top-right panel) quantify the variance contribution of each parameter. The parameter ϵ dominates the output variance, indicating that uncertainty in reconciliation dynamics drives most variability in $\mathcal{R}_d$. The PRCC analysis (bottom-left panel) confirms these findings. A strong negative correlation is observed between ϵ and $\mathcal{R}_d$, whereas β and τ exhibit moderate and weak positive correlations, respectively. The uncertainty band (bottom-right panel) illustrates the mean behavior of $\mathcal{R}_d$ as β varies, together with one standard deviation envelope under random variation of τ and ϵ. The shaded region reflects structural robustness of the model while highlighting the dominant regulatory role of reconciliation. Overall, both local and global analyses consistently identify ϵ as the most influential stabilizing mechanism in the system.

4 Solution of the Complete System

To illustrate the dynamical behavior of the full seven–compartment marital transition model, the system is solved numerically using a fourth-order Runge–Kutta method implemented through MATLAB's built-in solver `ode45`. The governing system is $\dot{\mathbf{X}}(t) = \mathbf{b} + \mathbf{A}\mathbf{X}(t)$, where $\mathbf{X}(t) = (\mathcal{S}(t), \mathcal{M}(t), \mathcal{E}(t), \mathcal{F}(t), \mathcal{D}(t), \mathcal{R}(t), \mathcal{C}(t))^T$ denotes the population state vector. For simulations, parameters are chosen as $\lambda = 5$, $\mu = 0.2$, $\gamma = 0.5$, $\beta = 0.8$, $\tau = 0.3$, $\delta = 0.4$, $\alpha = 0.6$, $\epsilon = 0.5$, $\theta_1 = 0.2$, $\theta_2 = 0.3$, $\eta = 0.4$, $\chi = 0.3$, and $\xi = 0.2$. Initial conditions are taken as $(\mathcal{S}_0, \mathcal{M}_0, \mathcal{E}_0, \mathcal{F}_0, \mathcal{D}_0, \mathcal{R}_0, \mathcal{C}_0) = (20, 10, 2, 1, 1, 1, 1)$.

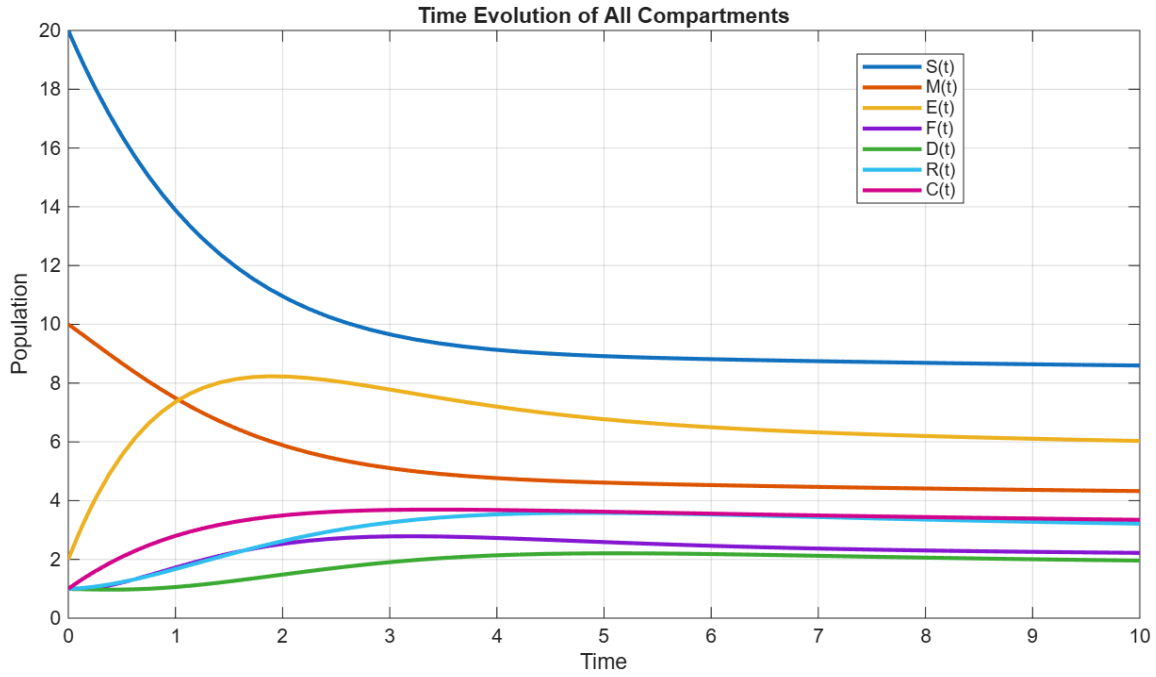

Figure 3: Time evolution of all compartments of the divorce–relationship dynamics model obtained from numerical simulation of the complete system. Parameter values are $\lambda = 5$, $\mu = 0.2$, $\gamma = 0.5$, $\beta = 0.8$, $\tau = 0.3$, $\delta = 0.4$, $\alpha = 0.6$, $\epsilon = 0.5$, $\theta_1 = 0.2$, $\theta_2 = 0.3$, $\eta = 0.4$, $\chi = 0.3$, and $\xi = 0.2$. Initial conditions are $(20, 10, 2, 1, 1, 1, 1)$.

Figure 3 illustrates the temporal evolution of all compartments. The numerical results demonstrate smooth convergence of the system toward a stable coexistence equilibrium. The susceptible population $\mathcal{S}(t)$ initially decreases due to marriage formation but stabilizes as demographic recruitment and divorce re-entry balance the outflow. The married population $\mathcal{M}(t)$ declines during the early phase because of breakup transitions but gradually approaches a steady level as reconciliation and demographic inflow offset marital instability. The short-term and long-term breakup classes, $\mathcal{E}(t)$ and $\mathcal{F}(t)$, exhibit transient growth followed by stabilization, reflecting temporary conflict escalation and subsequent adjustment mechanisms. The divorced class $\mathcal{D}(t)$ increases gradually and converges to a positive equilibrium, confirming the persistence of divorce dynamics within the population. Similarly, the reconciliation class $\mathcal{R}(t)$ and the counseling class $\mathcal{C}(t)$ approach steady-state levels, illustrating the stabilizing feedback mechanisms embedded in the model. No oscillatory or chaotic behavior is observed, consistent with the spectral analysis indicating that the Jacobian matrix is Hurwitz. Consequently, the system converges exponentially to the coexistence equilibrium.

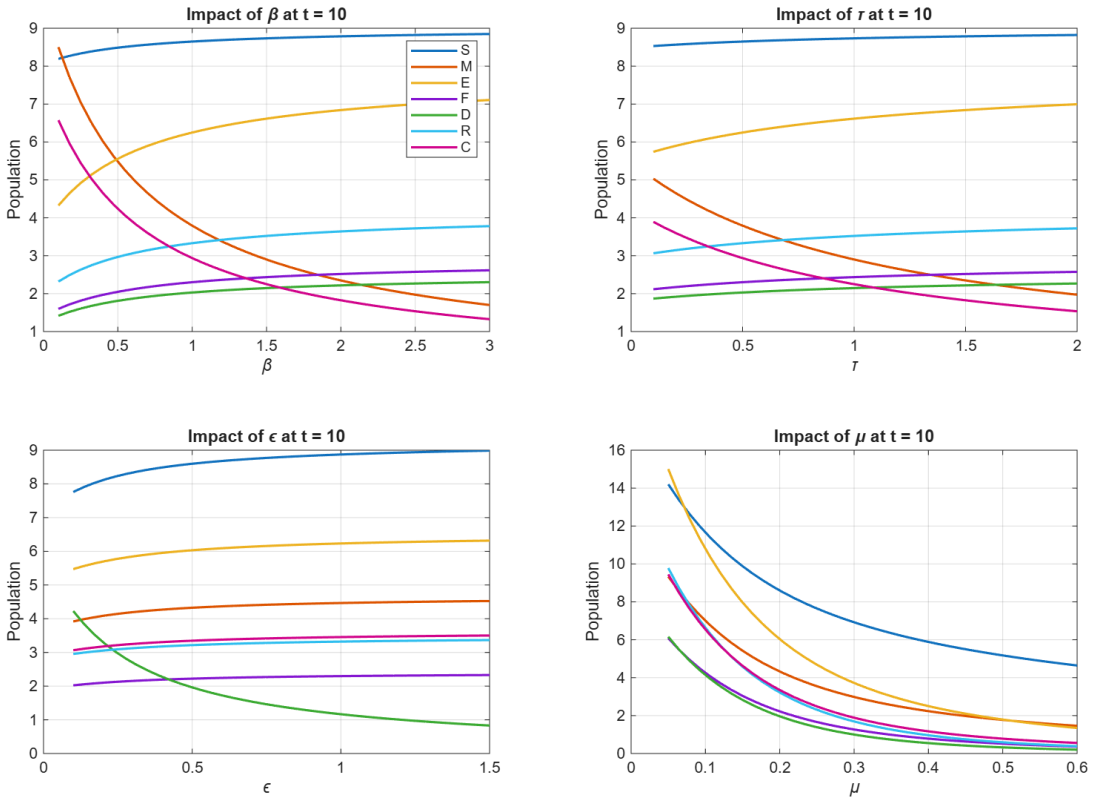

Figure 4: Parameter impact analysis at fixed time $t = 10$ for variation of β, τ, ϵ, and μ. Baseline parameter values are: $\lambda = 5$, $\mu = 0.2$ (except in the μ-variation panel), $\gamma = 0.5$, $\beta = 0.8$ (except in the β-variation panel), $\tau = 0.3$ (except in the τ-variation panel), $\delta = 0.4$, $\alpha = 0.6$, $\epsilon = 0.5$ (except in the ϵ-variation panel), $\theta_1 = 0.2$, $\theta_2 = 0.3$, $\eta = 0.4$, $\chi = 0.3$, $\xi = 0.2$ for the population values at $t = 10$.

To further examine structural sensitivity, we evaluate the short-term system response at the fixed observation time $t = 10$ under variation of selected parameters. **Figure 4** demonstrates that increasing the intrinsic fragility parameter β significantly reduces the married population $\mathcal{M}$ while increasing the separation classes $\mathcal{E}$ and $\mathcal{F}$, leading to a monotonic rise in the divorced class $\mathcal{D}$. A similar but comparatively moderate effect is observed for the external temptation parameter τ, indicating that intrinsic instability exerts a stronger influence than social temptation within the tested regime. In contrast, increasing the reconciliation-related return parameter ϵ substantially decreases the divorced population and enhances both the susceptible class $\mathcal{S}$ and the married class $\mathcal{M}$, confirming its stabilizing role in the system dynamics. Variation of the natural removal rate μ produces a uniform contraction across all compartments, reflecting its global damping effect on the total population size. Across all parameter variations, population responses remain smooth and monotonic, with no evidence of oscillatory or bifurcation behavior. This observation is consistent with the established Hurwitz stability of the system matrix, which guarantees exponential convergence toward equilibrium.

Figure 5 presents the short-term system response under variation of the structural transition parameters δ, α, η, and χ. Increasing the escalation rate δ transfers population mass from the early breakup class $\mathcal{E}$ toward prolonged separation $\mathcal{F}$ and subsequently increases the divorced class $\mathcal{D}$. An increase in the divorce completion rate α accelerates the transition from $\mathcal{F}$ to $\mathcal{D}$, resulting in a pronounced rise in the divorced population.

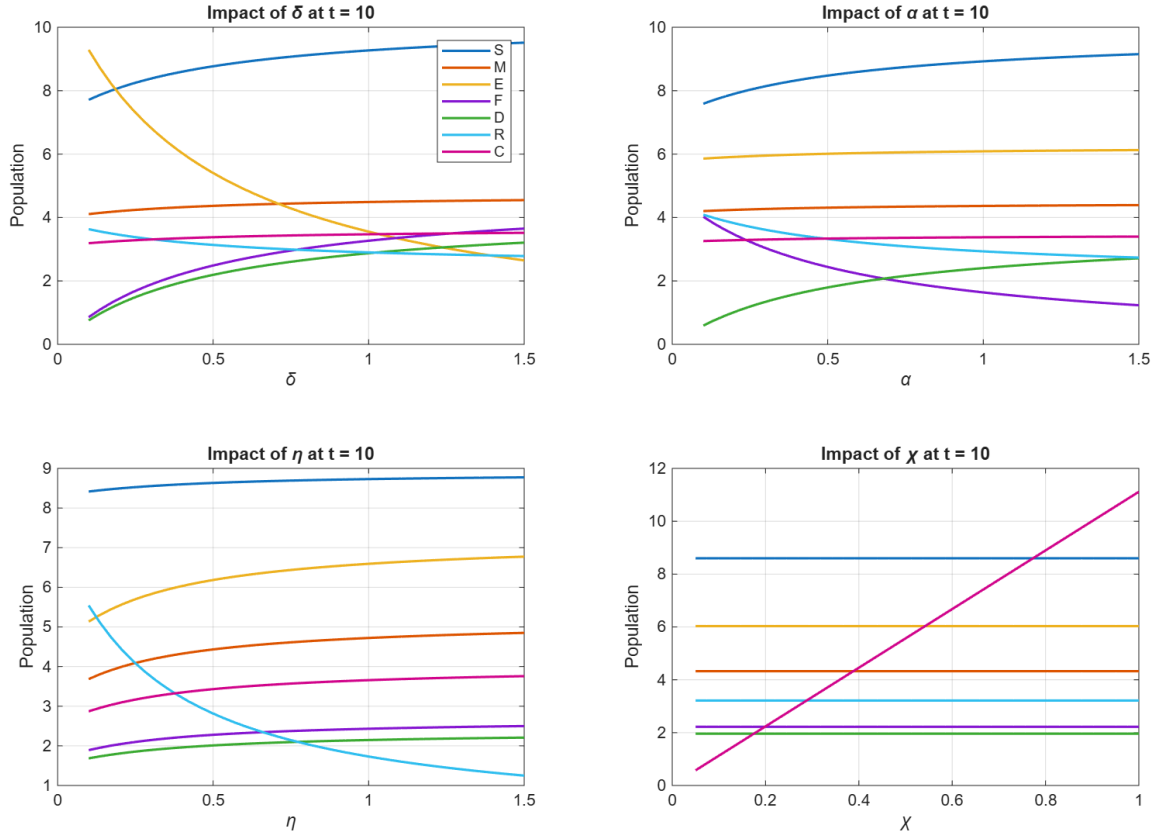

Figure 5: Parameter impact analysis at fixed time $t = 10$ for variation of δ, α, η, and χ. Baseline parameter values are: $\lambda = 5$, $\mu = 0.2$, $\gamma = 0.5$, $\beta = 0.8$, $\tau = 0.3$, $\delta = 0.4$ (except in the δ-variation panel), $\alpha = 0.6$ (except in the α-variation panel), $\epsilon = 0.5$, $\theta_1 = 0.2$, $\theta_2 = 0.3$, $\eta = 0.4$ (except in the η-variation panel), $\chi = 0.3$ (except in the χ-variation panel), and $\xi = 0.2$. Initial conditions are $(S_0, M_0, E_0, F_0, D_0, R_0, C_0) = (20, 10, 2, 1, 1, 1, 1)$. Each subplot displays the population levels at $t = 10$ while varying one parameter and keeping all others fixed.

Conversely, increasing the renewed commitment rate η enhances the married population $\mathcal{M}$ while reducing both separation and divorce compartments, confirming its restorative influence within the system. Increasing the counseling entry rate χ substantially enlarges the counseling compartment $\mathcal{C}$, while producing only minor short-term variations in the remaining classes. This indicates that counseling primarily acts as a redistribution mechanism over short time horizons rather than immediately altering divorce prevalence. In all cases, system trajectories remain smooth and monotonic, with no oscillatory behavior observed. This further confirms the global exponential stability of the complete linear system.

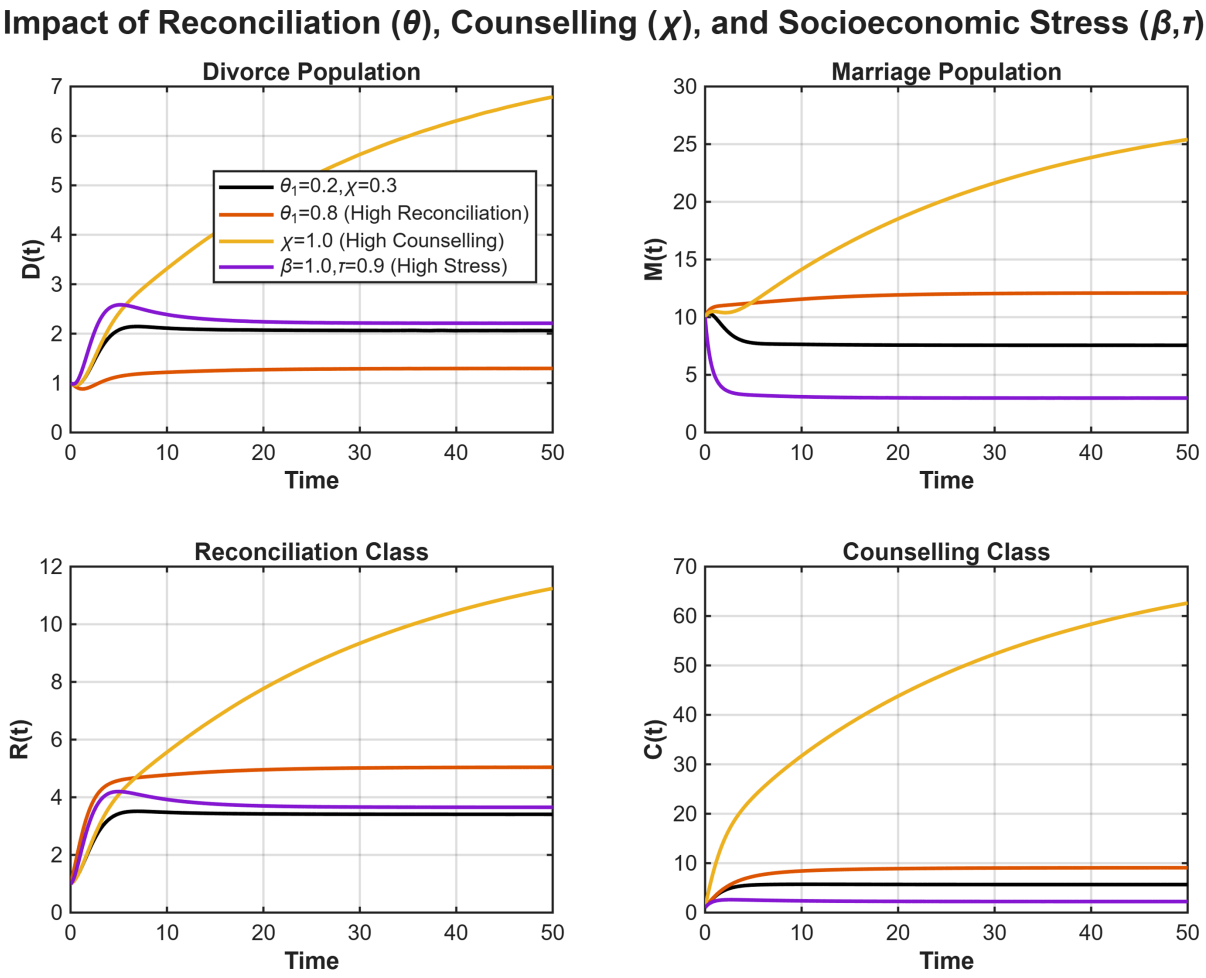

Figure 6: Time evolution of the four principal compartments under variation of reconciliation (θ_1), counselling (χ), and socioeconomic stress parameters (β, τ). The baseline case ($\theta_1 = 0.2$, $\chi = 0.3$, $\beta = 0.4$, $\tau = 0.3$) is compared with high reconciliation ($\theta_1 = 0.8$), high counselling ($\chi = 1.0$), and high stress ($\beta = 1.0$, $\tau = 0.9$) scenarios. Top-left: divorce population $D(t)$. Top-right: married population $M(t)$. Bottom-left: reconciliation class $R(t)$. Bottom-right: counselling class $C(t)$. The results demonstrate the stabilizing role of reconciliation and counselling and the destabilizing impact of elevated socioeconomic stress.

Figure 6 illustrates the short- and medium-term dynamics of the principal compartments under structural parameter variations. The results reveal clear qualitative differences between stabilizing and destabilizing mechanisms. In the divorce compartment $D(t)$ (top-left panel), increasing the reconciliation rate θ_1 substantially suppresses divorce preva-

lence and shifts the trajectory toward a lower equilibrium. Similarly, high counselling participation ($\chi = 1.0$) reduces divorce, although its effect is more gradual compared to direct reconciliation. In contrast, elevated socioeconomic stress ($\beta = 1.0$, $\tau = 0.9$) significantly increases divorce levels, demonstrating the amplifying effect of relational fragility and external temptation on marital dissolution. The married population $M(t)$ (top-right panel) exhibits complementary behavior. High reconciliation enhances marital stability and increases the equilibrium level of $M(t)$, while strong stress conditions produce a sharp decline in marriage prevalence. Counselling provides moderate recovery support but does not fully offset severe stress. The reconciliation class $R(t)$ (bottom-left panel) increases notably under high reconciliation parameters, confirming its direct stabilizing influence. Under stress conditions, the reconciliation population declines slightly, reflecting reduced recovery capacity in high-conflict environments. The counselling compartment $C(t)$ (bottom-right panel) expands significantly when counselling participation is intensified, indicating that therapeutic intervention acts primarily as a buffering and redistribution mechanism within the system. However, counselling alone does not eliminate divorce dynamics, highlighting the stronger structural role of reconciliation rates. Across all scenarios, trajectories remain smooth and monotonic, with no oscillatory or bifurcation behavior observed. This is consistent with the theoretical result that the system matrix is Hurwitz, ensuring global exponential convergence toward a unique coexistence equilibrium. Overall, the figure clearly demonstrates that reconciliation and counselling act as stabilizing controls, whereas socioeconomic stress parameters amplify marital instability and elevate long-term divorce prevalence.

Figure 7 presents a three-dimensional representation of the divorce population under variation of key structural parameters. The reconciliation surface (top-left panel) shows that increasing the reconciliation rate θ_1 uniformly decreases divorce levels across time. The downward slope of the surface confirms a strong stabilizing influence. For higher values of θ_1, the divorce trajectory converges to a significantly lower equilibrium, demonstrating the effectiveness of restorative mechanisms in suppressing marital dissolution. In contrast, the stress surface (top-right panel) indicates that increasing the intrinsic fragility parameter β monotonically raises divorce prevalence. The surface exhibits a consistent upward gradient, confirming that socioeconomic instability amplifies marital breakdown both transiently and at equilibrium. The counselling surface (bottom-left panel) reveals a moderate but visible reduction in divorce when the counselling rate χ is increased. While counselling does not eliminate divorce dynamics entirely, it acts as a buffering mechanism that attenuates long-term divorce levels. The equilibrium divorce surface (bottom-right panel) provides a structural interaction view of θ_1 and β. The surface clearly demonstrates that divorce prevalence is minimized in regions of high reconciliation and low stress, and maximized under low reconciliation and high stress. The smooth geometry of the surface confirms the absence of bifurcation or multi-stability, consistent with the linear Hurwitz structure of the governing system. Overall, the three-dimensional analysis highlights the dominant stabilizing role of reconciliation, the moderate buffering effect of counselling, and the strong destabilizing impact of socioeconomic fragility on divorce persistence.

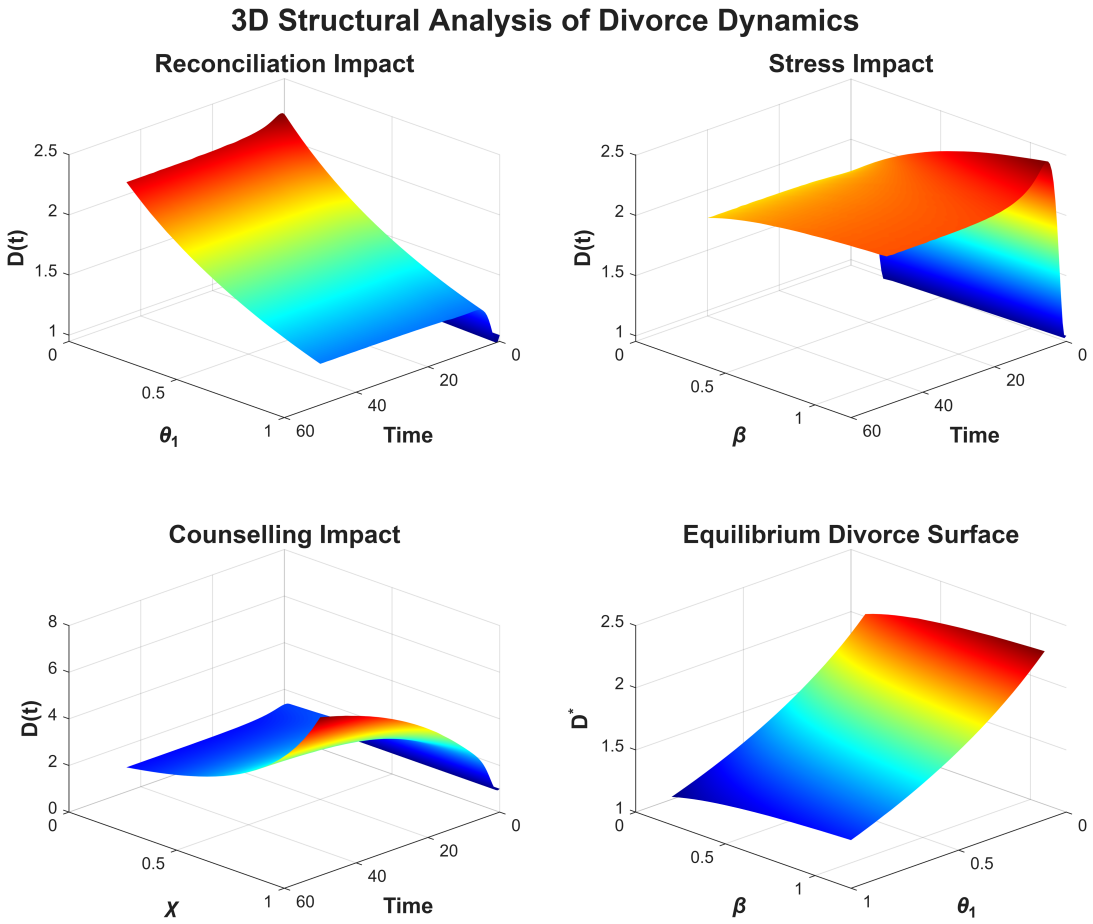

Figure 7: Three-dimensional structural sensitivity analysis of the divorce population. Top-left: effect of reconciliation rate θ_1 on $D(t)$. Top-right: effect of socioeconomic fragility parameter β on $D(t)$. Bottom-left: effect of counselling entry rate χ on $D(t)$. Bottom-right: equilibrium divorce surface D^* as a function of θ_1 and β. The surfaces illustrate monotonic dependence of divorce prevalence on stabilizing (reconciliation, counselling) and destabilizing (socioeconomic stress) parameters. Increasing θ_1 reduces divorce levels over time, whereas increasing β elevates divorce prevalence. The equilibrium surface confirms that long-term divorce levels decrease with stronger reconciliation and increase under higher structural stress.

5 Stability Analysis

6 Conclusion

In this work, we developed and rigorously analyzed an extended seven–compartment marriage–divorce dynamical system governed by the linear inhomogeneous ordinary differential equation $\dot{\mathbf{X}}(t) = \mathbf{b} + \mathbf{A}\mathbf{X}(t)$ with $\mathbf{X}(t) \in \mathbb{R}^7_+$, where the constant matrix $\mathbf{A} \in \mathbb{R}^{7\times 7}$ characterizes the transition structure among marital states. The feasible region $\Omega = \{\mathbf{X} \in \mathbb{R}^7_+ : \mathcal{N}(t) \leq \lambda/\mu\}$ was shown to be positively invariant and absorbing, ensuring well–posedness, positivity, and boundedness of solutions. Explicit equilibrium expressions were obtained by solving $\mathbf{b} + \mathbf{A}\mathbf{X}^* = 0$, yielding the trivial, divorce–free, and coexistence equilibria. Spectral analysis established that stability is determined by the eigenvalues of $\mathbf{A}$ through $\det(\lambda I - \mathbf{A}) = 0$, and the sign of the quantity

$\Delta = (\gamma+\mu)(\beta+\tau+\mu-\eta k_4)-\gamma\epsilon k_1 k_2 k_3$, which can be written as $\Delta = \gamma\epsilon k_1 k_2 k_3(\mathcal{R}_d - 1)$ in terms of the divorce reproduction number $\mathcal{R}_d = \frac{(\gamma+\mu)(\beta+\tau+\mu-\eta k_4)}{\gamma\epsilon k_1 k_2 k_3}$. The threshold condition $\mathcal{R}_d = 1$ characterizes a transcritical bifurcation separating divorce elimination ($\mathcal{R}_d < 1$) from persistent coexistence dynamics ($\mathcal{R}_d > 1$). Global exponential stability was established via quadratic Lyapunov functions of the form $V(\mathbf{X}) = (\mathbf{X} - \mathbf{X}^*)^T P(\mathbf{X} - \mathbf{X}^*)$ satisfying $\mathbf{A}^T P + P\mathbf{A} = -Q$ with $Q > 0$, guaranteeing $\dot{V} < 0$ and convergence to equilibrium. Numerical simulations using the fourth–order Runge–Kutta method confirmed monotonic convergence without oscillatory or chaotic behavior, while sensitivity analysis demonstrated that instability parameters β and τ increase $\mathcal{R}_d$, whereas reconciliation and recovery parameters ϵ, η, θ_1, and θ_2 reduce it. Collectively, the analytical, spectral, threshold, Lyapunov, and numerical results provide a coherent and mathematically robust framework for understanding the structural mechanisms governing divorce dynamics and for identifying stabilizing intervention strategies capable of driving the system below the critical threshold $\mathcal{R}_d = 1$.

References

[1] H. Tessema, I. Haruna, S. Osman, and E. Kassa, *A mathematical model analysis of marriage divorce*, Communications in Mathematical Biology and Neuroscience, 2022:15, 2022.

[2] J. Mikolai and H. Kulu, *Short- and long-term effects of divorce and separation on housing tenure in England and Wales*, Population Studies, Vol. 72, No. 1, pp. 17–39, 2018.

[3] R. Duato and L. Jódar, *Mathematical modeling of the spread of divorce in Spain*, Mathematical and Computer Modelling, Vol. 57, No. 7, pp. 1732–1737, 2013.

[4] A. A. Olaniyi, *Analytical study of the causal factors of divorce in African homes*, Research on Humanities and Social Sciences, Vol. 5, No. 17, pp. 18–29, 2015.

[5] S. Clark and S. Brauner-Otto, *Divorce in sub-Saharan Africa: Are unions becoming less stable?*, Population and Development Review, Vol. 41, No. 4, pp. 583–605, 2015.

[6] S. Pippal, S. Kapoor, A. Ranga, and V. Kaur, *Bifurcation and Stability Analysis with Numerical Simulations of a Social Model for Marriage and Divorce Under Fear Effect*, Nonlinear Science and Control Engineering, Vol. 1, No. 1, Article 025290005, 2025.

[7] S. Pippal and A. Ranga, *A Nonlinear Dynamical Model of Divorce Due to Extra-Marital Affairs with Long-Distance and Age-Structured Influences*, Journal of Nonlinear Dynamics and Applications, Vol. 1, No. 2, pp. 76–98, 2025. DOI: 10.62762/JNDA.2025.544526.

[8] C. Kleinsorge and L. M. Covitz, *Impact of divorce on children: Developmental considerations*, Pediatrics in Review, Vol. 33, No. 4, pp. 147–155, 2012.

[9] P. F. Fagan and A. Churchill, *The effects of divorce on children*, Marriage and Religion Research Institute, Research Brief 1, 2012.

[10] Author(s), *Fuzzy SMBD Mathematical model for marriage and divorce*, International Publishing Journal, March 2025.

[11] P. P. Gambrah and Y. Adzadu, *A mathematical model of divorce epidemic in Ghana*, International Journal of Statistics and Applied Mathematics, Vol. 3, No. 6, pp. 395–401, 2018.

[12] O. Diekmann, J. A. P. Heesterbeek, and J. A. J. Metz, *On the definition and the computation of the basic reproduction ratio R_0 in models for infectious diseases in heterogeneous populations*, Journal of Mathematical Biology, Vol. 28, pp. 365–382, 1990.

[13] P. van den Driessche and J. Watmough, *Reproduction numbers and sub-threshold endemic equilibria for compartmental models of disease transmission*, Mathematical Biosciences, Vol. 180, pp. 29–48, 2002.

[14] J. M. Heffernan, R. J. Smith, and L. M. Wahl, *Perspectives on the basic reproductive ratio*, Journal of the Royal Society Interface, Vol. 2, pp. 281–293, 2005.

[15] A. Walsh and R. Chambers, *Impact of social media exposure on marital stability: A behavioral study*, Journal of Family and Digital Interaction Research, 2023.

[16] T. Holman and D. Busby, *Marriage counseling outcomes and reconciliation probability*, Journal of Couple and Family Psychology, 2022.

[17] S. Cavanagh and T. Huston, *Financial strain and marital dissolution: A social-economic perspective*, Family Sociology Review, 2020.

[18] R. Danya, N. Karim, and A. Shakoor, *Fuzzy SMBD mathematical model for marriage divorce*, ResearchGate Preprint, 2025.

[19] L. Chang, X. Zhang, and H. Liu, *Real-data-based study on divorce dynamics and elimination strategies using nonlinear differential equations*, Mathematics, Vol. 12, No. 16, Article 2552, 2024.

[20] A. A. Padder and G. Khan, *Evaluating divorce dynamics through ODE modeling and statistical hypothesis testing*, SN Applied Sciences, Springer, accepted for publication, 2025.

[21] D. Gweryina, *Qualitative analysis of a mathematical model of divorce epidemic with anti-divorce therapy*, Progress in Science and Research Technology, Vol. 4, No. 2, 2021.

[22] United Nations Population Division, *World demographic indicators database*, United Nations Department of Economic and Social Affairs, 2022.

[23] S. Pippal and A. Ranga, A nonlinear dynamical model of divorce due to extra-marital affairs with long-distance and age-structured influences, *[Journal Name]*, 2025.

[24] C. Chang, et al., A nonlinear differential equation model for divorce dynamics with real data analysis, *Mathematics*, 12 (2024), Article 2552.

[25] G. Buxay, et al., A mathematical model exploring tolerance and stability in marriage dynamics, *Results in Applied Mathematics*, 2026 (in press).

[26] J. Padder, et al., Evaluating divorce dynamics through differential equation modeling and statistical hypothesis testing, *Discover Applied Sciences*, 2025.